

**SURFACE MODIFIED ZEOLITE CATALYSTS FOR THE  
HYDROUS PYROLYSIS OF HEAVY OIL**

BY

**Umer Khalil Chaudhry**

A Thesis Presented to the  
DEANSHIP OF GRADUATE STUDIES

**KING FAHD UNIVERSITY OF PETROLEUM & MINERALS**

DHAHRAN, SAUDI ARABIA

In Partial Fulfillment of the  
Requirements for the Degree of

**MASTER OF SCIENCE**

In

**CHEMICAL ENGINEERING**

**November 2015**

KING FAHD UNIVERSITY OF PETROLEUM & MINERALS

DHAHRAN- 31261, SAUDI ARABIA

**DEANSHIP OF GRADUATE STUDIES**

This thesis, written by **Umer Khalil Chaudhry** under the direction his thesis advisor and approved by his thesis committee, has been presented and accepted by the Dean of Graduate Studies, in partial fulfillment of the requirements for the degree of **MASTER OF SCIENCE IN CHEMICAL ENGINEERING.**



Dr. Mohammed Ba-Shammakh  
Department Chairman



Dr. Salam A. Zummo  
Dean of Graduate Studies



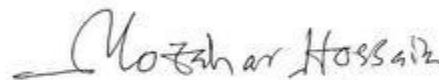
10/2/16  
Date



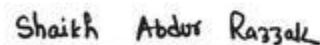
Dr. Dr. Adnan M. Al-Amer  
(Advisor)



Dr. Dr. Oki Muraza  
(Co-Advisor)



Dr. M. Mozahar Hossain  
(Member)



Dr. Shaikh Abdur Razzak  
(Member)



Dr. Zuhair Omar Malaibari  
(Member)

© Umer Khalil Chaudhry

2015

## DEDICATION

[This work is dedicated to my beloved parents.]

## ACKNOWLEDGMENTS

I would like to acknowledge all committee members for their support and guidance throughout my research work. I want to express my sincere and deepest gratitude to Supervisors, **Dr. Adnan Al Amer**, and **Dr. Oki Muraza** for their guidance and also keeping me motivated to achieve this milestone. I would also like to thank Center of Research Excellence in Nanotechnology (CENT), Chairman Dr. Zain Yamani and his team for providing me all facilities and support to complete this work in allocated time. I also thank to Chemical System Engineering Laboratory members Hokkaido University Japan for their sincere contributions in this work.

I am very grateful to **King Fahd University of Petroleum & Minerals (KFUPM)** for giving me this opportunity and all faculty members of Chemical Engineering department. Lastly, all my gratitude to my family: my **mother**, my **father** and my siblings for their love, patience, encouragement and prayers.

# TABLE OF CONTENTS

ACKNOWLEDGMENTS.....	V
TABLE OF CONTENTS.....	VI
LIST OF TABLES.....	IX
LIST OF FIGURES.....	X
LIST OF ABBREVIATIONS.....	XIII
ABSTRACT.....	XV
ABSTRACT (ARABIC).....	XVII
CHAPTER 1.....	1
INTRODUCTION .....	1
1.1 The World oil scenario .....	2
1.2 Upgrading of heavy oil .....	4
1.3 Carbon Rejection processes .....	5
1.4 Gasification .....	6
1.5 Delayed coking.....	6
1.6 Fluid coking and flexicoking .....	6
1.7 Visbreaking .....	6
1.8 Hydrogen addition process .....	7
1.9 Fluid catalytic cracking .....	7
1.10 Composition of heavy oil .....	8
1.11 Zeolites.....	9

1.12	Building Units for Zeolite Frameworks.....	9
1.13	Faujasite (FAU) .....	12
1.14	Mordenite (MOR) .....	13
1.15	Beta Polymorphs BEA and BEC .....	14
1.16	Chemistry of cracking catalysts.....	15
1.17	Solid silica and alumina chemistry .....	16
1.18	Mechanism of catalytic cracking reactions .....	19
<b>CHAPTER 2.....</b>		<b>21</b>
<b>LITERATURE REVIEW .....</b>		<b>21</b>
2.1	Hydrous pyrolysis of heavy oil: background .....	21
2.2	Catalytic hydrous pyrolysis.....	22
2.3	Catalyst Selection.....	26
2.4	Applications .....	27
2.5	Stability of zeolites in aqueous environment .....	27
2.6	Hydrophobic Zeolites .....	29
2.7	Organo-silane treated zeolite catalysts .....	33
2.8	Objective.....	36
<b>CHAPTER 3.....</b>		<b>37</b>
<b>METHODOLOGY AND EXPERIMENTAL.....</b>		<b>37</b>
3.1	Surface modification of catalyst using silane compound .....	37
3.2	Vapor phase silane treatment.....	37
3.3	Liquid phase silane treatment.....	38
3.4	Steam assisted catalytic cracking of heavy oil .....	38
3.5	Characterization of catalysts .....	41

<b>CHAPTER 4.....</b>	<b>42</b>
<b>VAPOR PHASE SILANE TREATED CATALYSTS .....</b>	<b>42</b>
4.1 Effect of silane treatment on catalysts properties.....	43
4.2 Effect of surface modified catalyst on cracking of AR .....	46
4.3 Effect of reaction time on the stability of parent and modified catalyst.....	54
<b>CHAPTER 5.....</b>	<b>58</b>
<b>LIQUID PHASE SILANE TREATED CATALYSTS.....</b>	<b>58</b>
5.1 Effect of silane treatment on catalyst properties .....	58
5.2 Effect of surface modified catalyst on cracking of AR .....	61
5.3 Effect of reaction time on cracking of AR .....	65
5.4 Comparison between Vapor phase and liquid phase silane treated catalyst .....	69
<b>CHAPTER 6.....</b>	<b>72</b>
6.1 Conclusions .....	72
6.2 Recommendations .....	73
<b>REFERENCES.....</b>	<b>74</b>
<b>VITAE.....</b>	<b>79</b>

## LIST OF TABLES

Table 1. Worldwide residue processing capacity (Mbbbl/day) .....	5
Table 2. Technologies for processing heavy oil [4].....	7
Table 3. Heavy oil feedstocks properties (www.total.com).....	8
Table 4. Properties of Beta zeolite.....	14
Table 5. Highlight of some catalytic hydrous pyrolysis of heavy oil. ....	23
Table 6. Steam-assisted catalytic cracking over metal oxide catalysts.....	25
Table 7. Silane treated zeolites and their application. ....	35
Table 8. Textural properties of parent and modified BEA catalyst using vapor silane treatment. ....	45
Table 9. Textural properties of parent and silane treated BEA catalysts.....	60

## LIST OF FIGURES

Figure 1. Total oil reserves: an overview [1].	2
Figure 2. Building units of zeolite structure from eight tetrahedra forming cube [6].	10
Figure 3. L to R: Double 4-ring, double 6-ring, Sodalite or beta cage [6].	10
Figure 4. Zeolites pore size distribution.	11
Figure 5. Mesoporous structure pore size range.	12
Figure 6. Building unit of FAU zeolite structure [6].	13
Figure 7. Structure of Beta zeolite.	15
Figure 8. Different ways of zeolite modification.	32
Figure 9. Schematic overview of hydrophobic zeolite in heavy oil upgrading.	33
Figure 10. Experimental setup of fixed-bed flow reactor.	40
Figure 11. XRD patterns of (a) BEA-Silane treated and (b) BEA-Parent.	43
Figure 12. NH <sub>3</sub> -TPD profiles of BEA-Parent and BEA-silane treated zeolite catalysts.	44
Figure 13. FT-IR spectra of pyridine-adsorbed (a) BEA-Parent and (b) BEA-Silane treated zeolite catalysts.	45
Figure 14. N <sub>2</sub> adsorption isotherms of BEA-Parent and BEA-Silane treated.	46
Figure 15. Carbon yield after 2 h reaction of AR with steam over BEA-parent and BEA-silane treated catalysts.	48
Figure 16. Gas composition (mol/g-AR) after 2 h reaction of AR with steam over BEA-parent and BEA-silane treated catalysts.	48
Figure 17. Molecular weight distribution of liquid product after 2 h reaction time.	49
Figure 18. Physical appearance of liquid product after 2 h reaction time over (a) BEA-parent and (b) BEA-silane treated catalysts.	50
Figure 19. N <sub>2</sub> adsorption isotherms of spent BEA-Parent-2h (after recalcination) and BEA-parent.	51
Figure 20. N <sub>2</sub> adsorption isotherms of spent BEA-silane treated-2h(after recalcination) and BEA-silane treated	52
Figure 21. XRD patterns (a) BEA-silane treated-2h (b) BEA-parent-2h (c) BEA-Parent.	52

Figure 22. Carbon yield after 4 h reaction of AR with steam over BEA-parent and BEA-silane treated catalysts.....	53
Figure 23. Gas composition (mol/g-AR) after 4 h reaction of AR with steam over BEA-parent and BEA-silane treated catalysts. ....	53
Figure 24. Molecular weight distribution of liquid product after 4 h reaction time. ....	54
Figure 25. Physical appearance of liquid product after 4 h reaction time over (a) BEA-parent and (b) BEA-silane treated catalysts.....	56
Figure 26. XRD patterns of (a) spent BEA-silane treated-4h (b) spent BEA-parent-4h (c) BEA-parent. ....	57
Figure 27. XRD patterns of (a) BEA- Liquid Silane treated and (b) BEA-Parent. ....	59
Figure 28. N <sub>2</sub> adsorption isotherms of BEA-Parent and BEA-Liquid silane treated. ....	60
Figure 29. NH <sub>3</sub> -TPD profiles of BEA-Parent and BEA-Liquid-silane treated zeolite catalysts.....	61
Figure 30. Carbon yield after 2 h reaction of AR with steam over BEA-parent and BEA-Liquid phase silane treated catalysts. ....	63
Figure 31. Gas composition (mol %) after 2 h reaction of AR with steam over BEA-parent and BEA-Liquid phase silane treated catalysts.....	63
Figure 32. Molecular weight distribution of liquid product over BEA-Parent and BEA-Liquid silane treated catalysts after 2 h reaction time.....	64
Figure 33. Physical appearance of liquid product after 2 h reaction time over (a) BEA-parent and (b) BEA-Liquid silane treated catalysts. ....	65
Figure 34. Physical appearance of liquid product after 4 h reaction time over (a) BEA-parent and (b) BEA-Liquid silane treated catalysts. ....	67
Figure 35. Gas composition (mol %) after 4 h reaction of AR with steam over BEA-parent and BEA-Liquid phase silane treated catalysts.....	67
Figure 36. Molecular weight distribution of liquid product over BEA-Parent and BEA-Liquid silane treated catalysts after 4 h reaction time.....	68
Figure 37. XRD patterns of (a) BEA-Vapor silane treated-4h (b) BEA-Parent-4h (c) BEA-Liquid silane treated-2h (d) BEA-Parent.....	69
Figure 38. Comprison of lighter hydrocarbon yield over vapor silane treated and liquid silane treated catalysts for 2h and 4h reaction times.....	70

Figure 39. Physical appearance of liquid product after 2 h reaction time over (a) BEA-  
parent (b) BEA-Liquid silane treated and (c) BEA-Vapor silane treated  
catalyst. .... 71

## LIST OF ABBREVIATIONS

API	:	American Petroleum institute
AR	:	Atmospheric Residue
Atm	:	Atmosphere
BAS	:	Brønsted Acid Sites
BEA	:	Beta Zeolite
cP	:	CentiPoise
DRIFT	:	Diffuse reflectance infrared Fourier transform
EIA	:	Energy Information Administration
FAU	:	Faujasite
FCC	:	Fluid Catalytic Cracking
FID	:	Flame Ionization Detector
GC	:	Gas Chromatography
H/C	:	Hydrogen/Carbon
HDT	:	Hydrotreater
HDC	:	Hydrocarking
IGCC	:	Integrated Gasification Combined Cycle
LAS	:	Lewis Acid Sites

Mol		Mole
MOR	:	Mordenite
MR	:	Membered ring
MW		Molecular weight
OPEC	:	Organization of the Petroleum Exporting Countries
TCD	:	Thermal Conductivity Detector
TPD	:	Temperature Programmed Desorption
WGSR	:	Water Gas Shift Reaction
USY	:	Ultra stable Zeolite Y
XRD	:	X-ray Diffraction

## ABSTRACT

Full Name : Umer Khalil Chaudhry  
Thesis Title : Surface modified zeolite catalysts for the hydrous pyrolysis of heavy oil  
Major Field : Chemical Engineering  
Date of Degree : November 2015

Surface of the Beta zeolite catalyst ( $\text{SiO}_2/\text{Al}_2\text{O}_3=150$ ) was modified to improve its hydrophobicity and stability using organo-silane compound. Triphenyl silane was deposited on external surface of catalysts through two techniques i.e. vapor phase deposition and liquid phase deposition. Characterization techniques such as XRD, TPD,  $\text{N}_2$ -adsorption and FT-IR pyridine were used to characterize these catalysts. Silane treated Beta catalysts retained its crystallinity after modification however, decrease in acidity were observed in  $\text{NH}_3$ -TPD studies. These results were confirmed by FT-IR pyridine analysis which showed decrease in both Brønsted and Lewis acid site after modification. Parent Beta and silane treated Beta catalysts were tested in fixed-bed reactor for steam-assisted catalytic cracking of atmospheric residue. Silane treated Beta zeolites exhibited hydrophobic properties; hence the modified Beta catalysts were more stable at high temperature in aqueous environment. It was found that the Beta catalysts modified through both techniques retained their crystallinity and phase purity after reaction. Moreover coke formation was also reduced significantly over silane treated Beta catalysts. This indicates the increase in the stability of catalysts. Furthermore, lighter

hydrocarbons yield from 2 h reaction time were higher as compared to reaction time of 4 h. Yield of gases, gasoline (C<sub>7</sub>-C<sub>13</sub>) and gas oil (C<sub>14</sub>-C<sub>20</sub>) over a vapor phase silane treated Beta zeolite catalyst were 11.6 mol %, 55.7 mol % and 3.7 mol % respectively for 2 h reaction time.

## ABSTRACT (ARABIC)

الاسم الكامل: عمر خليل شودري

عنوان الرسالة: تعديل سطوح المواد الحفازة الزيوليتية للإنحلال الحراري المائي من النفط الثقيل

التخصص: الهندسة الكيميائية

تاريخ الدرجة العلمية: نوفمبر 2015

تم تعديل سطح المحفز الزيوليتي من نوع بيتا زيولايت (نسبة جزيئات السيلكا إلى الألومنيوم=150) لتحسين سطحه لمقاومة الماء واستقراره باستخدام المركب العضوي السيلاني. تم غرس المركب العضوي ثلاثي فينيل السيلاني على السطح الخارجي من محفزات البيتتا من خلال تقنيتين هما الترسيب في الحالة البخارية و الترسيب في الحالة السائلة. واستخدمت التقنيات التالية لتوصيف الزيولايت مثل حيود الأشعة السينية، و الإمتصاص الحراري المبرمج، و مقياس مساحة السطوح و حامضية السطوح لتوصيف هذه المحفزات.

محفز بيتتا المعدل بالمركب العضوي السيلاني احتفظ بالبلورات الأساسية للمحفز بعد التعديل، ومع ذلك، لوحظ انخفاض في نسبة الحموضة في دراسات مقياس حامضية السطوح. وتم تأكيد هذه النتائج عن طريق تحليل البيريدين FT-IR والتي أظهرت انخفاضا في كل من موقع حمض برونستيد ولويس بعد التعديل.

تم اختبار محفز بيتتا الزيولاتي قبل و بعد إضافة المركب العضوي السيلاني في مفاعل ثابت مستمر و في وجود البخار لمساعدة التكسير التحفيزي. و حيث ظهر جليا، أن المحفز المعدل بالمادة السيلانية أصبح يحمل ميزة مقاومة الماء و بالتالي كانت محفزات بيتتا المعدلة أكثر استقرارا في درجة حرارة عالية في بيئة مائية.

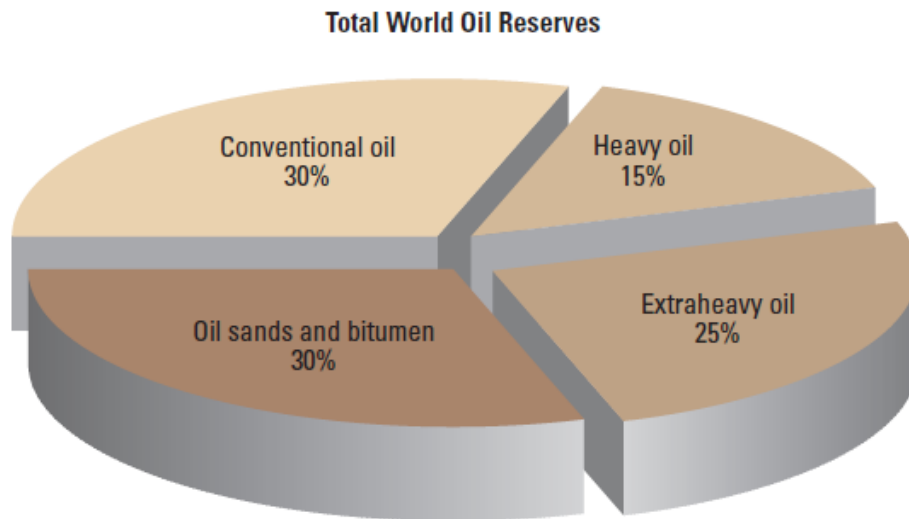
وقد وجد أن المحفزات بيتتا المعدلة سواء من خلال التقنيتين احتفظت بتبلورها و نقاء المادة بعد التفاعل. وعلاوة على ذلك تم تخفيض تكون الفحم بشكل كبير في حال التحسين بالمركب السيلاني. وهذا يدل على زيادة في استقرار المواد الحفازة. علاوة على ذلك، كان ناتج المركبات الهيدروكربونية الخفيفة خلال ساعتين من التفاعل كان أعلى مقارنة مع أربع ساعات من التفاعل. وكان الناتج من الغازات، البنزين (C7-C13) والقازولين (C14-C20) في حال وجود المحفز بيتتا المعالج بالسيلانين هو 11.6 مول٪، 55.7 مول٪ و 3.7 مول٪ على التوالي لمدة ساعتين من التفاعل.

# **CHAPTER 1**

## **INTRODUCTION**

The subject of unconventional fossil fuels got more importance in last few decades as conventional fossil fuels reserves are near depletion. Proven reserves which include conventional crude oil are 1.47 trillion bbl and according to study these reserves will sustain up to next forty years at the current level of production [1]. So developing new technologies to utilize unconventional oil resources such as shale oil, tar sand and extra heavy oil is the demand of time.

Unconventional fossil fuel resources makes 70 % of the total world's oil reserves [1] (Figure.1). Fuel from unconventional oil is only accountable for 12 % of total fuel supply [2]. Huge investment and attention should be dedicated towards developing economical and feasible technologies to explore and utilize these unconventional resources.



^ Total world oil reserves. Heavy oil, extraheavy oil and bitumen, make up about 70% of the world's total oil resources of 9 to 13 trillion bbl.

Figure 1. Total oil reserves: an overview [1].

## 1.1 The World oil scenario

Venezuela, Saudi Arabia and Canada are leading countries in the world with proven oil reserves of 20%, 18% and 12% respectively (OPEC) [2]. According to U.S Energy administration association, Saudi Arabia is the largest oil producing country with the production of more than 10 million bbl/day. Proven reserves of conventional oil are 1.47 trillion barrels which are enough for next 40 years with current rate of production. But considering the increasing consumption of oil, conventional oil resources are depleting and production rate declining 5 % annually. In near future world oil scenario will be shifting towards unconventional oil reserves. According to US-energy administration association study Canada heavy oil reserves are ranked second as compared to conventional oil reserves in Saudi Arabia. While Canada and Venezuela combined have more oil reserves in the category of heavy oil.

Total 30 countries are found to have heavy oil reserves in considerable amount United States (California), Mexico, Brazil, Russia, Indonesia, China, Colombia, Ecuador, Iraq, Kuwait, Saudi Arabia, Chad and Angola ([www.halliburton.com](http://www.halliburton.com)). Reserves of heavy oil in these countries make 20 % of total oil reserves of world which is equivalent to 15 years addition of oil supply. Middle East alone have 78 billion barrel of heavy oil reserves which is recoverable and this amounts 3.5 time the U.S total reserves ([www.wsj.com](http://www.wsj.com)). Although Middle East especially Saudi Arabia is depending on easy extracting light oil which is of very high quality but it is expected a transformation from conventional to unconventional oil as lighter oil reserves will not last for too long. Hence, many research on processing and digging out heavy oil is under way in this part of region. According to the International Energy Agency (IEA), approximately 8 trillion dollars will be spent by 2040 in order to develop new oil fields to meet the increasing energy demand in our world. This demand will partially be met by heavy oil and bitumen resources worldwide which are estimated to be approximately 6 trillion barrels.

Saudi Arabia has one fifth of proven conventional oil reserves. Although these reserves are enough to sustain for many upcoming years but after Canada and Venezuela, Saudi Arabia is also targeting to hit heavy oil reserves to enhance their production. Also much advancement is made globally to process heavy oil. Refinery processes are needed to convert heavy crude into valuable products like middle distillates and gasoline.

## 1.2 Upgrading of heavy oil

Current Oil refining technologies are best optimized to give improved yield and high quality products. Heavy oil have low economic value and more difficult to process as compared to lighter oil. Among all the refining technologies, handling of residue oil is most important and difficult. Economies of an operating refinery majorly depend upon their utilization of heavy oil residues. A substantial investment has been poured into the upgradation of heavy oil processing like Saudi Aramco world largest oil refinery is contributing their efforts to minimize heavy residue. Generally, heavy oil upgrading technologies divided into two categories, Hydrogen addition or carbon rejection. Some technologies based on both carbon rejection and hydrogen addition. Carbon rejection technology because of its low investment presents 56 % of total heavy oil processing capacity. However some countries like Japan largely depends upon hydro treating technologies. Both these technologies are targeted to increase hydrogen to carbon ratio. Carbon rejection technology is oldest and comparatively easier which operates at high temperatures to thermally degrade larger molecules. At the same time molecules combine together to form even heavier molecules resulting in coke formation. These technologies include visbreaking, flexi coking, delayed coking, fluid coking etc. As these processes require less investment and operating cost but on the other hand many disadvantages are associated with these processes such as fewer yields to lighter component, coke formation and presence of other components (S, N) in end products [3]. On the other hand hydrogen addition processes give more product yield as compared to carbon rejection processes. Addition of hydrogen increases H/C ratio hence decrease the density which results in the products of higher commercial values. Hydrogen addition

technologies classified on the type of reactor are fixed-bed, moving-bed, ebullated-bed and slurry-bed processes. Table 1 represents overview of residue processing capacities.

**Table 1. Worldwide residue processing capacity (Mbbbl/day)**

<b>Technology</b>	<b>United states</b>	<b>Europe</b>	<b>Canada/ Venezuela</b>	<b>Japan</b>	<b>Rest of World</b>	<b>World total</b>	<b>% capacity</b>
<b>Carbon rejection</b>							
Cracking/Visbreaking	44	2260	331	24	1635	4293	25.8
Coking	2245	673	951	66	1169	5104	30.7
Total	2289	2933	1282	90	2804	9397	56.5
<b>Hydrogen addition</b>							
Fixed-bed, HDT	499	149	30	591	1042	2312	13.9
Ebullated-bed, HDC	102	79	244	23	49	497	2.99
Slurry-phase, HDC			4			4	0.02
Residue FCC	831	681	281	318	1832	3942	23.7
Total	1432	909	559	932	2923	6755	40.6
<b>Others</b>							
Deasphalting	283	46	39	16	75	458	2.76
Total	4002	3889	1879	1037	5801	16609	100.00

### 1.3 Carbon Rejection processes

Thermal processes or carbon rejection processes involves transfer of hydrogen from the heavy molecules to the lighter molecules resulting in coke formation.

## **1.4 Gasification**

This process is carried out temperature above 1000 °C major products are syngas, ash and carbon. However modified technology named integrated gasification combined cycle (IGCC) has showed great potential for electricity generation due to their minimal effects on environment.

## **1.5 Delayed coking**

This technology is widely used in many refineries because of low initial investments. This technology has an ability to handle any type of residue. Disadvantages of this technology are high coke formation and less liquid yield.

## **1.6 Fluid coking and flexicoking**

These two technologies are developed from fluid catalytic cracking. Flexi coking is the extended form of fluid coking. Liquid yield in these processes are little higher as compare to delayed coking.

## **1.7 Visbreaking**

Visbreaking is developed technology used for both atmospheric and vacuum residues. This is accompanied by thermal cracking to reduce the consumption of fuel oil.in this

process residue is heated upto 500 °C and then cracked at lower residence time to avoid coke formation.

## 1.8 Hydrogen addition process

Hydrogen addition process usually involves catalysts. Fluid catalytic cracking is one example of such processes.

## 1.9 Fluid catalytic cracking

Fluid catalytic cracking offers higher gasoline yield as compare to any other processes. But one disadvantage of this process is the requirement of high quality feed with less metal and sulfur contents. Therefore, atmospheric residue is only suitable for this process. This process use acidic catalyst like USY zeolites. A short overview of heavy oil processing technologies is shown in Table 2.

Table 2. Technologies for processing heavy oil [4]

Catalytic processing technologies	Thermal processing technologies
Ebullating bed residue hydroprocessing technology	Visbreaking
Moving/ebullated bed residue catalytic process	Thermal coking
Fixed bed residuum or vacuum residuum desulfurization	Delay coking

	Gasification
--	--------------

### 1.10 Composition of heavy oil

Heavy oil is differentiated on the basis of high viscosity and low API gravity compared to conventional oil. Definition of heavy oil according to World Petroleum council is oil whose viscosity is between 100 cP and 10,000 cP at reservoir temperature with API gravity between 10 and 20 [3]. Heavy oil has component with complex structure and it is difficult to understand the composition of heavy oil. Many researches have been carried out to understand the heavy oil composition. Asphaltenes are present in heavy oil are most complex and highly aromatic compound. Asphaltenes and resins are usually responsible of high viscosity. In addition to complex compounds heavy oil contains sulfur, nitrogen and other compounds. Composition of these compounds depends upon the origin of heavy oil [4, 5].

Higher viscosity and specific gravity of oil makes it different from conventional lighter oil. Based on viscosity and API gravity heavy oil is divided into three categories as shown in Table 3.

**Table 3. Heavy oil feedstocks properties (www.total.com)**

	<b>API gravity</b>	<b>Viscosity (cP)</b>
<b>Heavy oil</b>	18-25	10 – 100
<b>Extra heavy oil</b>	Up to 20	10000

<b>Oil sands and bitumen</b>	7-9	Above 10000
------------------------------	-----	-------------

### 1.11 Zeolites

Zeolites are subset of molecular sieve family and their structure is based on  $AlO_4$  and  $SiO_4$  tetrahedral framework connected to each other by sharing Oxygen atoms. Its framework structure has voids and channels occupied by cation, water molecules and other guest species.



M is univalent charge balancing cation, x is number of framework aluminum atom, t is total number of framework tetrahedral atom [6]. Zeolites have wide application at industrial scale because of its large surface area, high thermal stability and strong acidity. [7]

### 1.12 Building Units for Zeolite Frameworks

The building block in a zeolite is a tetrahedron where Si or Al is surrounded by oxygen atoms. Combining these building blocks in different arrangements gives many frameworks of zeolite with different morphologies, pore dimensions and unique characteristics. For example, eight-tetrahedron structure connects by sharing oxygen atoms form a cube (Figure. 2). This cube will be a building unit for more complex structures and form cavities and pore openings. This cube can also be designated as a double four ring structure hence if basic building units combine in a way that it form hexagonal prism like structure, double six-ring will be generated (Figure.3).

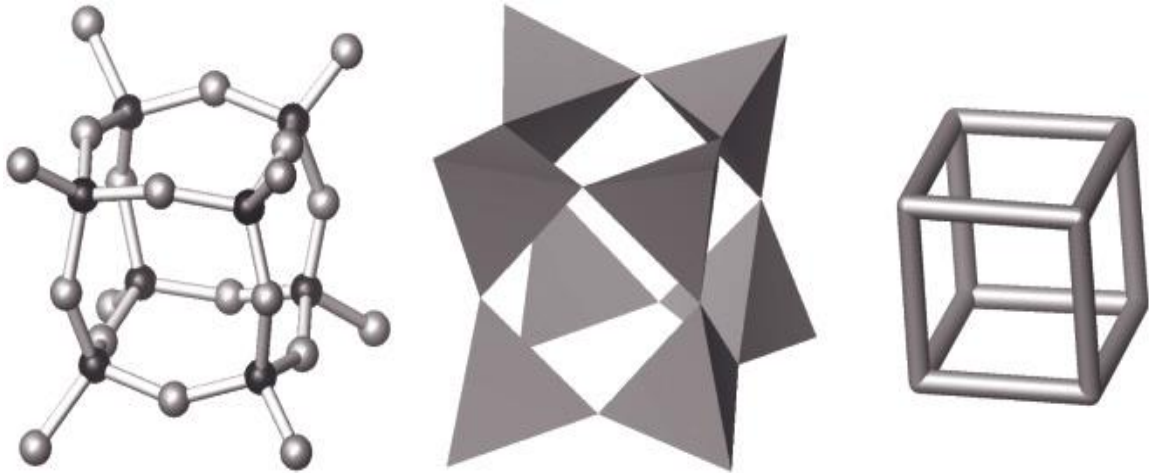


**Figure 2. Building units of zeolite structure from eight tetrahedra forming cube [6].**

In most literature, framework is represented by Si or Al atom linkages (Si-Si, Al-Al, Si-Al) while oxygen atom is considered at the center of link. The polyhedral building units have unique nomenclature such as sodalite cage or numerical codes i.e cube or  $4^6$  and hexagonal ring  $4^6 6^2$ . Figure. 3 represent the different building units of zeolite framework with their nomenclatures.



**Figure 3. L to R: Double 4-ring, double 6-ring, Sodalite or beta cage [6].**

‘n’ Number of rings where n defines the number of Si or Al atoms, defining the face of polyhedral building units are called pores. Pore size less than six-rings are called cages, because larger molecules cannot pass through these cages. If any of the pore size in polyhedral is larger than six-ring it is called cavities. Pores that are extended in one or

multi-dimensions and larger than six-ring are called channels. For instance, LTA structure contains two types of cages i.e.  $4^6$  and  $4^66^8$ , one type of cavity and eight-ring pore extended in three-dimensions. Diffusion and reaction of molecules in zeolites mainly depend upon pores size and channels dimension. Selection of zeolite is made on the type of reaction, product, reactant and diffusion limitations. Heavy hydrocarbon reactions usually involve large pore zeolite (MOR, BEA or FAU) in order to avoid diffusion limitation. Zeolite pore size distribution is shown in Figure.4 and Figure.5.

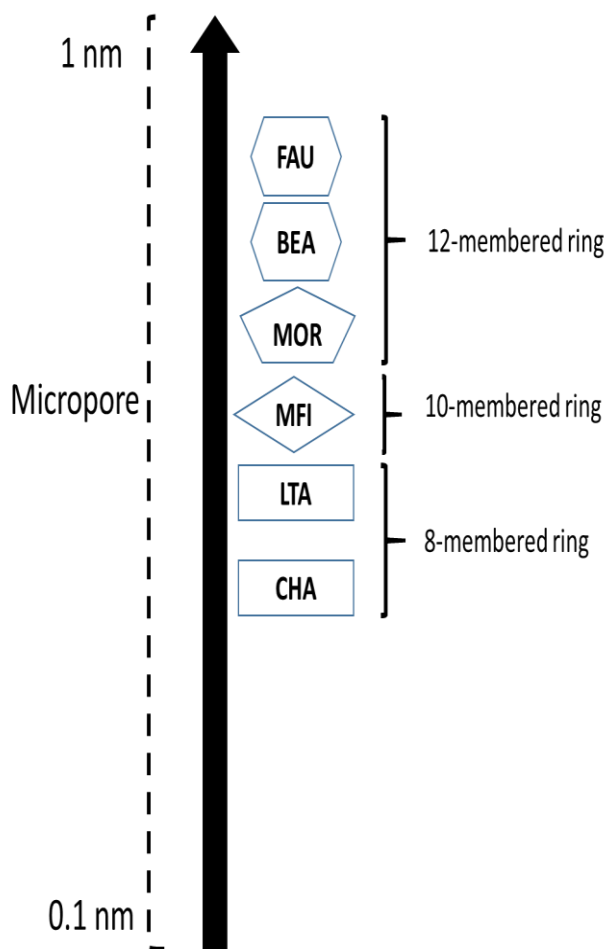


Figure 4. Zeolites pore size distribution.

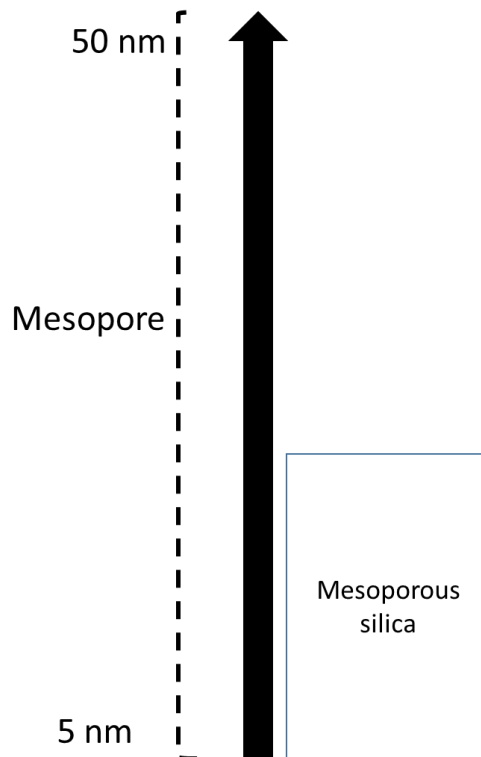
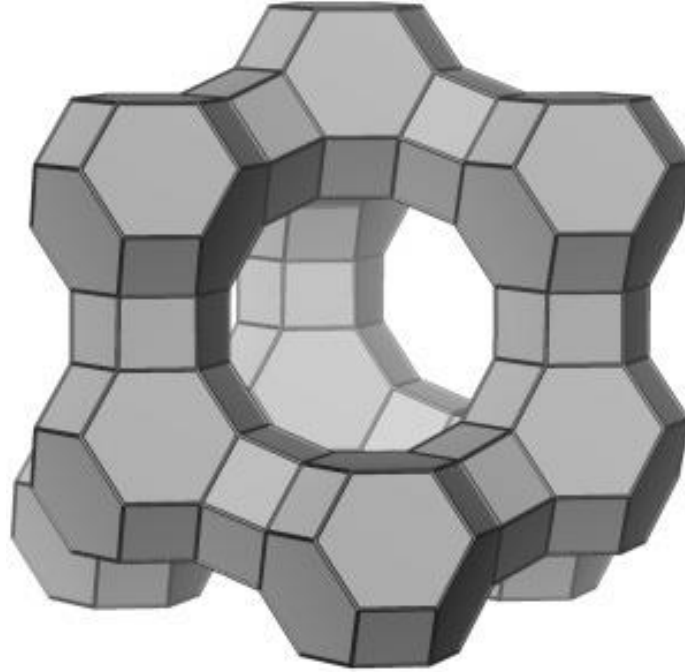


Figure 5. Mesoporous structure pore size range.

### 1.13 Faujasite (FAU)

FAU has three-dimensional structure connected by 12-ring pore systems. Sodalite cages are connected by six-rings which make a super cavity and FAU one of the large pores structure zeolite (Figure. 6). The unit cell formula of FAU zeolite can be written as  $| M_x (H_2O)_y | [Al_x Si_{192-x} O_{384}]$  where  $x$  is the number of Al atoms and  $M$  is a monovalent cation. The number of Al atoms can be varying from 96 to 4 (Si/Al ratio 1 to 50). FAU has further two types Zeolite X and Y. Zeolite X ranges between Si/Al ratios 1 to 1.5 and zeolite Y ranges between Si/Al ratios 96 to 77. Zeolite Y has special importance in industry because of its higher Si/Al ratio and higher activity.



**Figure 6. Building unit of FAU zeolite structure [6].**

### **1.14 Mordenite (MOR)**

Mordenite is widely used zeolite in practical application such as in catalysis, separation, adsorption, semiconductors, chemical sensors, and nonlinear optics. Mordenite has chemical formula  $\text{Na}_8 (\text{H}_2\text{O})_{24}[\text{Si}_{40}\text{Al}_8\text{O}_{96}]$  and parallel 12-membered ring (MR) channels (0.67 x 0.70 nm) along the c-axis direction, which were interconnected by 8-MR (0.34 x 0.48 nm) along b-axis [8-10]. Due to small size of 8-MR mordenite is considered as a one dimensional zeolite. Especially in adsorption and catalytic application it is treated as one dimensional. In addition high thermal stability and acid strength makes it more useful in industrial applications such as alkylation, hydro isomerization, reforming, dewaxing and cracking processes [10, 11].

## 1.15 Beta Polymorphs BEA and BEC

BEA refers as beta polymorph A, it has not been synthesized in its pure form yet. BEC refers to polymorph C, although it is synthesized in pure form but only as Ge polytype. Beta zeolite has three-dimensional 12-ring framework structure with elliptical opening 0.76x 0.64 nm (Figure.7). Beta zeolites are considered to be high Si/Al ratio framework zeolites. Its structure is highly disordered and has many internal defects which make its acidity properties more interesting. Table 4 represents the properties of Beta polymorph A.

**Table 4. Properties of Beta zeolite.**

<b>Type</b>	<b>Beta polymorph A</b>
Chemical Formula	[Na <sub>7</sub> ][Al <sub>7</sub> Si <sub>57</sub> O <sub>128</sub> ]
Pore structure	Three-dimensional 12-ring
Synthetic forms	Beta, Al-rich beta,CIT-6
Type	Beta polymorph A
Pore structure	Three-dimensional 12-ring
Synthetic forms	FOS-5,ITQ-14,ITQ-17

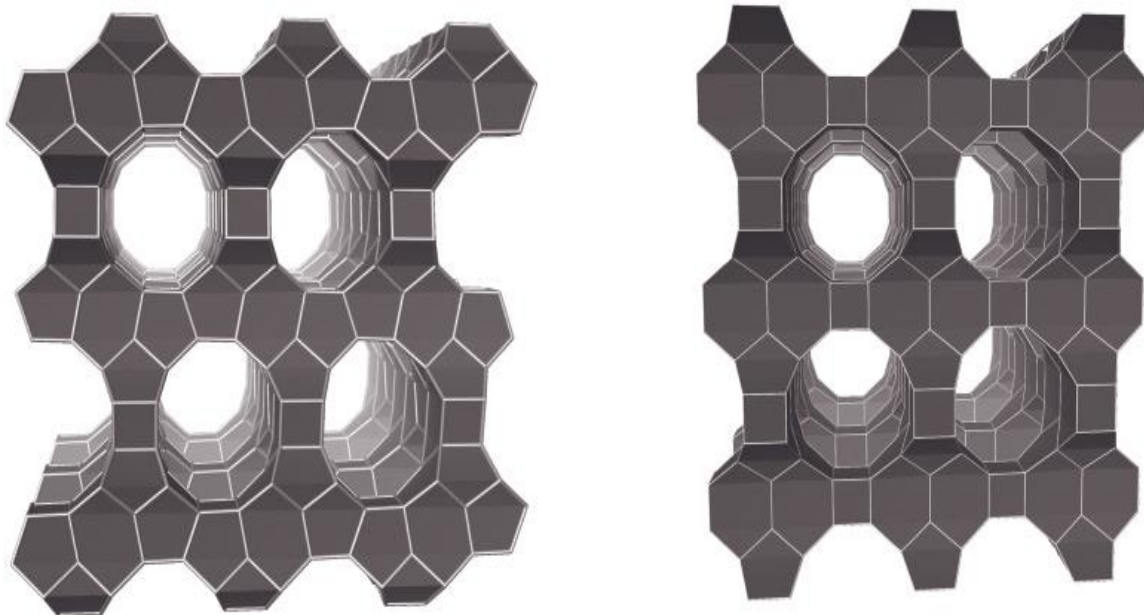


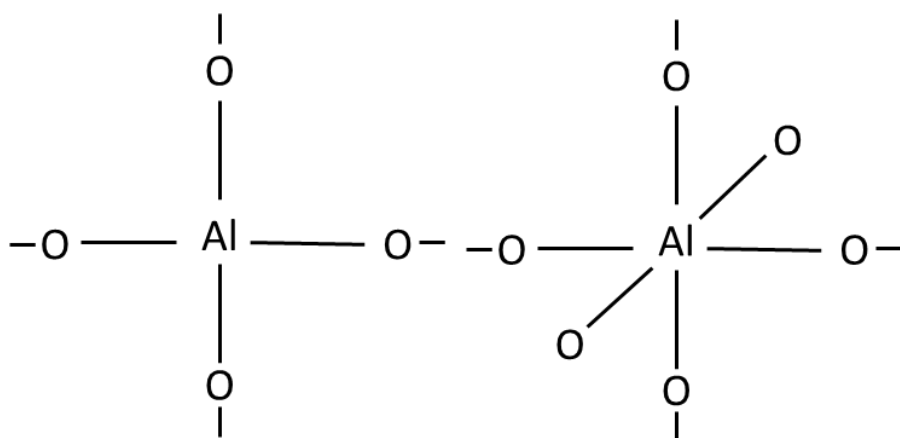
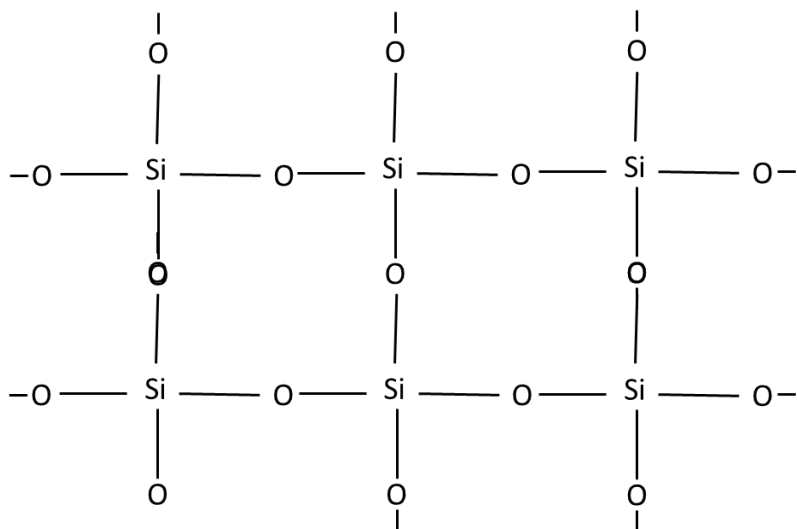
Figure 7. Structure of Beta zeolite.

## 1.16 Chemistry of cracking catalysts

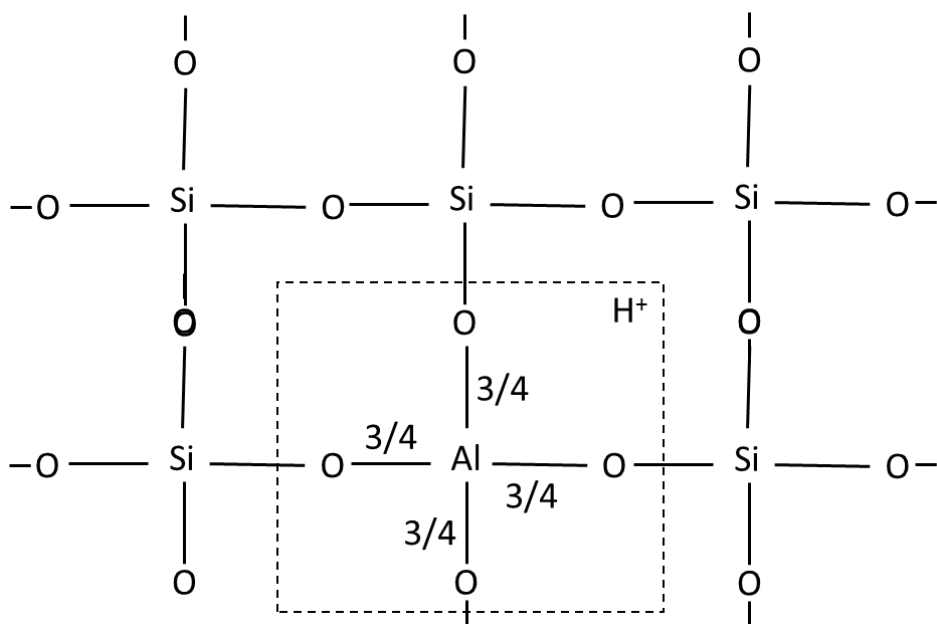
Chemistry of silica and alumina in solid state set a foundation for silica-alumina solid catalysts. Active parts in these catalysts formed when one aluminum atom shares four oxygen atoms and which further shared by four silicon atoms. Their combine structure generates a net positive charge which is compensated by cation which is  $H^+$  in most of the cases. Alone silica is either not active or slightly active. However, alumina alone has more activity than silica in cracking reaction but combination of silica-alumina generates highly active sites and generates solid-acid catalysts. Zeolites are important type solid-acid catalysts which have proven be to be most efficient catalyst in cracking reactions. It is important to first throw a light on the chemistry of silica and alumina in solids states and their role in cracking reactions.

## 1.17 Solid silica and alumina chemistry

There is no Si=O=Si bond exists in solid state, rather each silicon is surrounded by four oxygen atoms as shown in formula given below. Oxygen atoms are at the corners of tetrahedron and silicon in the center forms a basic building unit of crystalline structure of solid catalyst. Aluminum makes two structures with oxygen i.e. four oxygen atoms surrounding aluminum atom forms tetrahedral while six oxygen atoms generates octahedral structure presented in formula given below. Any of these two combinations may be a building unit of complex polymers. But silica-alumina cracking catalyst is a result of tetrahedrally linked alumina structures with silica tetrahedrons [12].



Cracking reaction mainly depends upon activity of catalyst which comes from  $H^+$  associated with every single unit of silica-alumina structure.

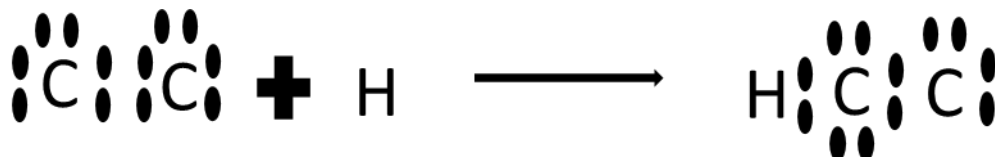


Formula above represents the silicon-oxygen tetrahedron network where each silicon satisfy its valance by sharing four oxygen atom while oxygen atom bonding with two silicon to satisfy its valance. When center silicon is replaced by tetrahedral aluminum atom it creates a net negative charge. Aluminum has valance of three which makes oxygen deficient of charge. Hence, AlO<sub>4</sub> part of structure is unsatisfied by one valance unit. This valance unit is compensated by H<sup>+</sup>. So it can be concluded from above discussion that positive charge hydrogen ion is a result of tetrahedral aluminum.

Catalyst activity is associated with its acidity; this means that maximum number of Si-O-Al bond gives higher acidity and hence higher activity. High silica to alumina ratio should give maximum acidity but this it is not possible to get maximum acidity. This is due to the formation of Si-O-Si bonds during synthesis of catalyst. This reduces potential Si-O-Al bond concentration.

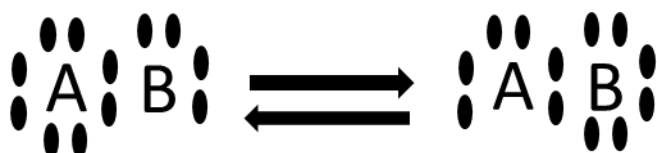
## 1.18 Mechanism of catalytic cracking reactions

It is well known that an acid catalyst involves carbonium ion reactions. Hydrocarbon cracking reactions in the presence of acid catalysts involve both carbonium ion and carbonions. Carbonium ions are formed from olefins.

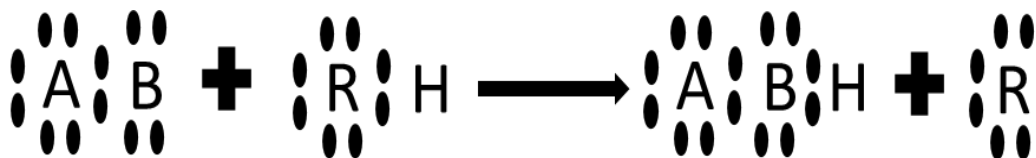


This reaction is the starting of cracking and follows different type of reactions which involves[12]:

**Type 1:** When carbonium ion B has greater affinity for electron than other molecule say A. hence electron moves to B and A becomes carbonium ion. This reaction was proposed by whitmore.



**Type 2:** carbonium ion reacts with a neutral molecule to become stable and form another carbonium ion. When the molecule is olefin, an unsaturated carbonium ion is formed.





## CHAPTER 2

### LITERATURE REVIEW

#### 2.1 Hydrous pyrolysis of heavy oil: background

In the introduction, many techniques have been discussed for the upgrading of heavy oil. All these techniques are already commercialized and contributing to meet the current demand of lighter hydrocarbons. Still many improvements in current technologies are required to meet the current demand for lighter fuels. Hydrous pyrolysis, also known as aquathermolysis, is an efficient technique for the cracking of hydrocarbon in presence of water. Hydrous pyrolysis process involves injection of superheated steam in a reactor to increase H/C ratio and reduces the viscosity of oil. Hyne was the first who reported that reduction of viscosity during hydrous pyrolysis process is mainly due to breakage of C-S bond as the breakage energy of C-S bond is lower than other bonds [13]. Hydrolysis of organosulfur compounds involves water gas shift reaction (WGSR) [14]. Hydrogen from water transfers to oil and results in the release of H<sub>2</sub>S after breaking C-S bond.



It was observed, hydrogen produced was responsible for oil upgrading and hence improve the quality of heavy oil. Carbon dioxide was also produced at steam injection temperature from metal carbonates present in oil reservoirs. Breakage of C-S bond plays decisive role in viscosity reduction and it was investigated that concentration, reactivity

and type of sulfur compounds also effect the viscosity reduction. Hence it is concluded that hydrous pyrolysis has many advantages [15, 16].

(a) Reduction of viscosity and hence improvement of its flow properties.

(b) Desulfurization.

(c) Hydrogenation and hence upgrading of heavy oils.

Purpose of hydrous pyrolysis is to decrease the asphaltenes and resins contents in heavy oil and increase H/C to resin and asphaltenes ratio. Hence reduces the viscosity and improves oil quality [17].

## **2.2 Catalytic hydrous pyrolysis**

During hydrous pyrolysis reaction long change molecules break and form radicals which take part in polymerization reaction and hence further increase viscosity. This problem can be overcome by using catalyst that hinders polymerization. Clark et al [18] first studied hydrous pyrolysis of heavy oil in the presence of catalyst. It was found that minerals present in well act as a catalyst during hydrous pyrolysis process. Higher viscosity reduction was observed in nickel and cobalt reactors than quartz reactor so keeping in this results further research was made in the presence of different catalysts. Kapadia et al reported that reactor material hastelloy also took part in reaction hence cracking results improved in the presence of hastelloy. Previously transition metals were employed as a catalyst for heavy oil cracking at higher pressure where hydrogenation and thermolysis gave conversion up to 56% [19]. Iron naphthenate in the presence of cyclohexane (hydrogen donor) was found to be more effective catalyst [20]. In the

presence of nickel and iron, hydrodesulphurization and hydrodenitrogenation are achieved during thermolysis. Hence, hydrous pyrolysis reaction initiated from the breakage of weaker C-S bond and C-O bonds. Moreover, increase in H/C ratio and decrease in O/C ratio was also reported as a result of catalytic hydrous pyrolysis reaction over sulfonic- $\text{H}_3\text{Po}_{12}\text{O}_{40}$  at 280 °C and 30 bar [21]. At Liaohe oil field in china, researchers investigated catalytic effect of hydrous pyrolysis on oil containing sulfur content as low as 0.5 wt % [17]. Hydrous pyrolysis catalysts can be divided in mineral water-soluble catalyst, oil-soluble catalysts, and dispersed catalyst. And these catalysts give different degree of viscosity reduction. Mineral < water-soluble< oil-Soluble < dispersed [15]. List of catalysts used for pyrolysis of heavy oil is given in Table. 5 and Table 6 presents the yields of lighter hydrocarbons over metal oxide catalysts during steam-assisted catalytic cracking of heavy oil.

**Table 5. Highlight of some catalytic hydrous pyrolysis of heavy oil.**

Catalyst	Temperature T (°C)	Time T (h)	Viscosity Reduction [%]	Conversion into lighter components [%]	References
Alkyl ester sulfonate copper	240	24	90.72	10.12	[22]
Nano-nickel catalyst	280	24	98.9		[23]

Without catalyst	240	24-72	28-42	-	[24]
Amphiphilic catalyst	200	-	96.26	C10< 3.73% to 51.54	[16]
Gemini catalyst	170	24	90	10	
Aromatic Sulfonic Iron and Aromatic Sulfonic Molybdenum	200	24	95.6 and 99.3 respectively		[17]
Dodecylbenzene Sulfonate and Nickel	85	120	73 and 79		[25]
Reservoir minerals	160-280	0-48	25.8	27.8 (saturated HC) and 32.2 (aromatics)	[26]
Ni, W, Mo and C catalysts	240	200	97		[27]

0.8% tetralin	240	24	80		[28]
Nano-keggin- K <sub>3</sub> PMo <sub>12</sub> O <sub>40</sub>	280	24	92.3		[29]
Aromatic sulfonic copper	280	24	95.5	13.72	[29]
Aromatic sulfonic H <sub>3</sub> PMo <sub>12</sub> O <sub>40</sub>	280	24			[30]
Ultra-sonic assistant and XAGD-2 catalyst	200	24	80.5		[31]

Table 6. Steam-assisted catalytic cracking over metal oxide catalysts.

Catalysts	Conditions	Feedstock	Conversion into lighter C <sub>7</sub> -C <sub>35</sub> ) (Mol %)
ZrO <sub>2</sub> -FeO <sub>x</sub> -Al <sub>2</sub> O <sub>3</sub>	500 °C for 2 h	Vacuum residue	C <sub>7</sub> -C <sub>18</sub> 56.3 %
FeO <sub>x</sub> -ZrO <sub>2</sub>	500 °C for 2h	Atmospheric residue	57 %

<b>FeOx</b>	500 °C for 2h	Atmospheric residue	50 %
<b>TiO<sub>2</sub>-ZrO<sub>2</sub></b>	470 °C for 2 h	Atmospheric residue	40 %

### 2.3 Catalyst Selection

As shown in Table 5, various type of catalysts were employed and different extent of viscosity reduction was achieved .Pore diameter, size, morphology and activity plays an important role in the selection of process. Zeolite catalysts as a most important industrial catalyst which have much application in cracking including FCC were not taken into consideration for hydrous pyrolysis up till now. Zeolite catalysts because of their higher activity, crystallinity and selectivity than other catalysts considered superior for many practical application but stability of zeolite in hot aqueous environment is always a question. Hydrothermal stable zeolite will be the breakthrough for the processes in the presence of water. Zeolites are mainly categorized base on Si/Al ratio: low, intermediate, high and silica molecular sieves. Low Si/Al ratio (1-1.5) zeolites have less acidity as compare to intermediate (2-5) and high (10-100) Si/Al ratio zeolites. Thermal stability and hydrophobicity also increases with increase Si/Al ratio. Properties associated with framework of Si/Al allow low and intermediate zeolites to remove water from organics in adsorption and catalysis while high and silica molecular sieves are used to remove organics from water because of their hydrophobic nature [7].

High intra crystalline surface area, uniform porous structure, micro- and meso-porous characteristics, wide range of crystal size, the ion exchange properties, high internal acid density, thermal stability and the ability to absorb chemicals into their structure introduced zeolites in commercial and practical applications [32].

## 2.4 Applications

Three main properties of zeolites make it commercially important [33];

- Ion exchange capacity for detergents
- Separation and adsorption because of their molecular sieve properties
- Catalysts because of their high acidity

Substitution of tetravalent silicon by trivalent aluminum in the framework gives rise to a net negative charge, which is compensated by cations, *e.g.*  $H^+$ ,  $Na^+$ , and  $Ca^+$ . If these cationic sites are exchanged to  $H^+$ , strong Brønsted acid sites are formed and these strong acid sites enable zeolite applications in catalysts. Many zeolites especially ZSM-5, FAU, Beta, Mordenite have found many commercial application in catalysts such as hydrocracking, catalytic dewaxing, fluid catalytic cracking, upgrading of naphtha and syn fuel production. Hence zeolite can be used to achieve stability, selectivity and yield [6, 11, 33, 34].

## 2.5 Stability of zeolites in aqueous environment

Zeolites has numerous applications as a catalyst, adsorbent etc. water-free environment cannot always be guaranteed, many catalytic applications involve steam or water at high or moderate temperature. Although zeolites are considered as stable material at high

temperature but stability in water at high temperature is still questionable. Many recent researches have been conducted to study the zeolite properties in aqueous environment. Zeolites that showed stable structure in water were found to distort in steaming environment. So, still lot of study is required to study the zeolite behavior in water and steam both. It was reported that degradation mechanism in water is hydrolysis of Si-O-Si bond while steaming cause dealumination (Si-O-Al) [35].

Recently extensive study on stability of zeolite Y in hot water shows that Si-O-Si bond is hydroxyl ion ( $\text{OH}^{-1}$ ) catalyzed and generated two silanol groups which further accelerates the degradation. Si-O-Al is attacked by proton but this reaction is dominant in steaming condition (dealumination). Hydrolysis of Si-O-Al extract Al from framework and form extra framework Al, defected structure left with four silanol groups Si-OH but these defects were healed by other silicon atom those were removed in process [35]. It was observed that removal of Al framework mostly occur during cooling step after steaming. Zeolite Y showed increase in degradation of structure with increasing Si/Al ratio which in opposite of other zeolites. It was also observed that EFAl results from dealumination helped to block further hydrolysis of Si-OH groups. This could be the one reason of high stability of low Si/Al zeolite Y. Moreover, Lanthanum incorporated in zeolite structure increased the stability of MTT zeolite in the presence of steam [36].

Five types of OH groups are associated with H-beta namely silanol OH, bridging hydroxyl, two type of AlOH, and hydrogen hydroxyl groups[37]. Brønsted acidity is because of bridging hydroxyl group and has a main role in many catalyzed reactions. Lewis acidity mainly depends upon the Extra framework aluminum (EFAL). Combination of two polymorph in beta zeolite results in the higher concentration of

structural defects [38]. Dealumination was found to be the main reason of structure degradation. Decrease in the concentration of BAS in both untreated and steamed BEA was low as expected. Decrease in the concentration of BAS after steaming was justified by removal of framework Al. However less concentration of BAS in untreated was because of charge neutralization of some  $\text{AlO}^{4-}$  by positively charge extra framework aluminum (EFAL). It should be clear that one EFAL result in the loss of two BAS, one by itself and other is by blocking framework Al. Moreover, EFAL are important for thermal stability as they cover framework Al and prevent further degradation [37].

In contrary to FAU (zeolite Y) and Beta (BEA), ZSM-5 found stable at 200 °C and 150 °C for 6 h [35]. No change in crystallinity and structural changes were observed. Some octahedrally coordinated Al removed which indicates the removal of some (EFAL) from the zeolite structure [35].

## **2.6 Hydrophobic Zeolites**

As discussed earlier, in aqueous environment zeolites leads to deactivation whether irreversible (dealumination) or reversible (deposition of solvent molecules on zeolites). It was also observed that in water, degradation of Si-O-Si bond is the main mechanism while in steam Si-O-Al bond breakage leads to deactivation. Recently many researches have been carried out to improve the stability of zeolite in aqueous phase. One major disadvantage of zeolite is reduction in crystallinity in hot water at high temperature (>150 °C) [39, 40]. Reducing the hydrophilicity is one solution to enhance zeolite tolerance at elevated temperature. Density of acid sites depends on the Si/Al ratio, framework configuration and type of cation. Similarly their stability is also depending upon these

factors. Increasing Si/Al ratio helps to improve the hydrophobic nature of zeolite but at the same time it also decreases Al framework which results loss of Brønsted acid sites (BAS). Sacrificing Brønsted acid sites which are responsible for catalytic reactions such as dehydration alkylation and oligomerization is not desirable outcome [41].

Studies have shown that purely siliceous surface are hydrophobic and hydroxyl site which includes Si-OH groups and Si-O-Al sites are hydrophilic and can easily attached by water. In the case of microporous materials (zeolites) higher increasing Si/Al ratio decreases water uptake. Mordenite zeolite of varying Si/Al ratio (80-200) showed hydrophobic nature with increasing Si content in structure [42]. Same trend was observed in mesoporous materials, MCM-41 and MCM-48 modified with trimethylsilane showed decrease in water uptake [43]. Large port zeolite e.g. FAU, BEA were found unstable in hot water even at temperature  $>150$  °C while at the same temperature in vapor phase structure was stable [35, 37]. Zapata et al observed highly hydrophilic structure of H-FAU, degraded in hot liquid water just after 3 h. H-FAU functionalized with organo-silane groups showed remarkable increase in hydrophobicity. Silane groups attached on the external surface of H-FAU prevented water molecules to attach and adsorb on internal surface. It was concluded that organo silane functionalization prevented contact of water with zeolite which otherwise cause irreversible structural degradation. MCM-41 functionalized with methyl, ethyl and phenyl groups were structurally more stable, indicating that siloxane hydrolysis rates were slower than pure silicious MCM-41.

Surface modification of zeolite with sodium fluoride, lanthanum, phosphorus and organo-silane (silanation) increase hydrophobicity without reducing the density of acid sites [44-49]. Cerqueira et al [47] studies effect of the introduction of phosphorus on H-MFI

zeolite before and after hydrothermal treatment. Introduction of pyridine and sodium fluoride to develop hydrophobic siliceous ferrierite was also reported elsewhere [46]. Impregnation of different Si/Al ratio ZSM-5 with phosphorus in  $H_3PO_4$  form was studied by Corma et al [44]. Figure. 8 shows the different routes to impart hydrophobic character in zeolites, whether by post treatment or in-situ synthesis methods.

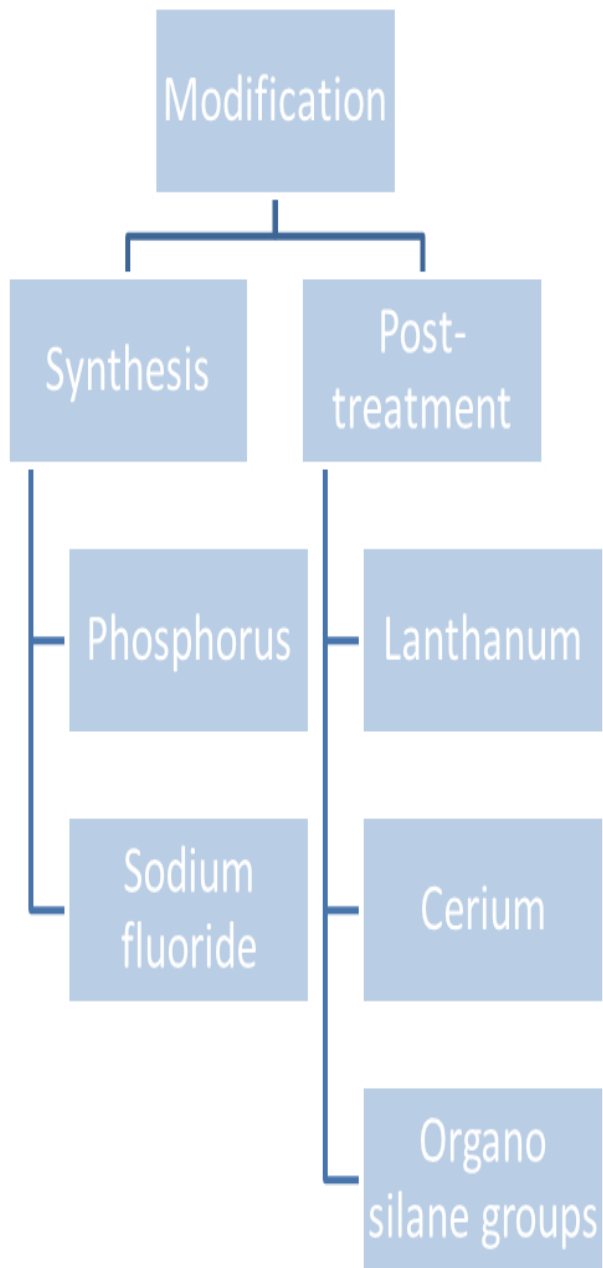


**Figure 8. Different ways of zeolite modification.**

## 2.7 Organo-silane treated zeolite catalysts

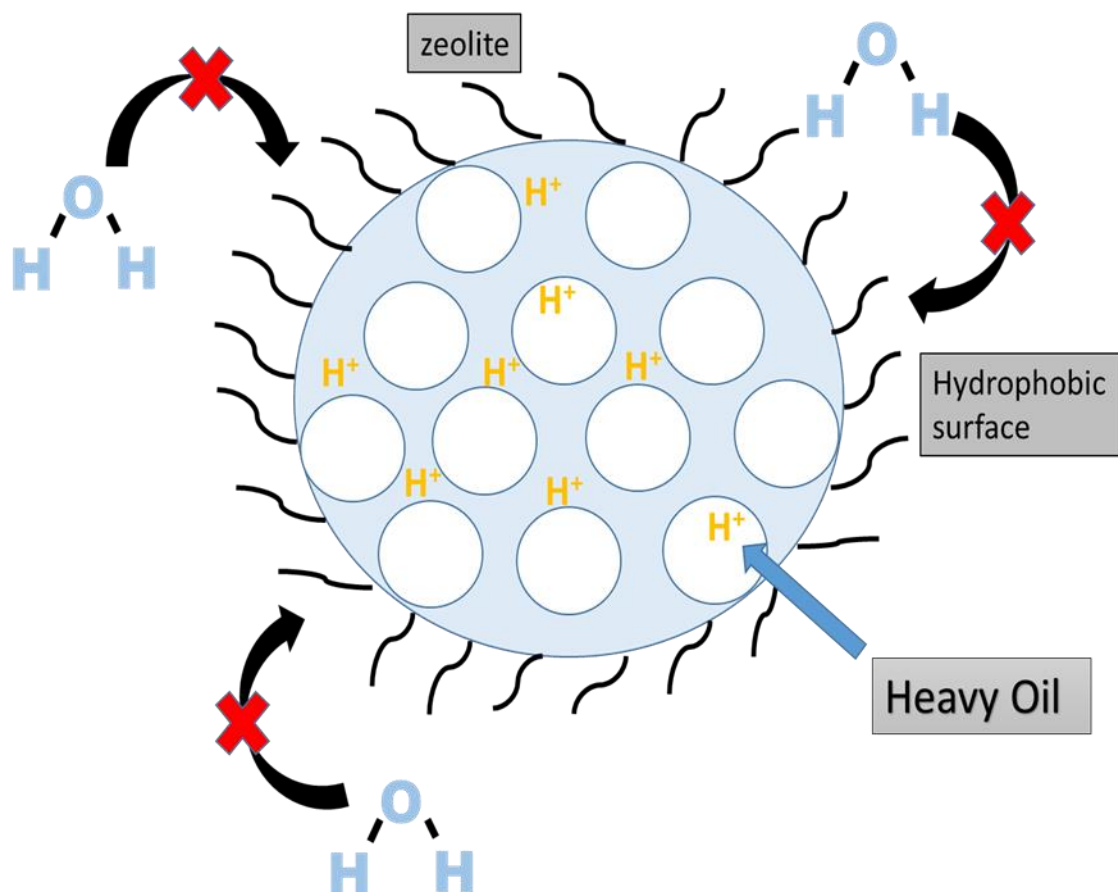


Figure 9. Schematic overview of hydrophobic zeolite in heavy oil upgrading.

In general activity, selectivity and stability depend upon composition and structure of zeolite, diffusion of reactants and products and post-treatment of synthesized zeolite. It is important to get desired properties of zeolite to achieve better results. There are many compounds and techniques are available in literature to modify zeolite in order to get desired properties. If application of zeolite is required in hot water then hydrophobicity and stability of zeolite plays an important role [39, 41]. One way to increase the hydrophobicity is to increase Si/ Al ratio or dealumination of zeolite but this also cost the loss of Brønsted acid site and as a consequence reduction in its catalytic activity [50, 51].

There are numerous applications of silane treated zeolites. Recently, silane compounds were used to control the activity of ZSM-5 zeolite catalyst. organo-silane compounds were employed in catalytic cracking of silane compound on zeolite surfaces. These silane compounds on calcination formed  $\text{SiO}_2$  units in external active site hence decreasing the activity but in increase in selectivity of lighter components [40]. Moreover, decreased acidity also caused to reduce coke deposition and increased the stability of ZSM-5. Same technique was used for n-hexane cracking over di-phenyl silane treated ZSM-22. Results showed higher selectivity of propylene and less aromatics [52]. More importantly stability of catalyst increased remarkably after and ZSM-22 found stable even after longer reaction time. This method involved chemisorption of silane compounds vapors on the external surface in  $\text{N}_2$  flow followed by decomposition of silane compounds on surface at  $550\text{ }^\circ\text{C}$ . finally these silane compounds formed  $\text{SiO}_2$  units on external active sites in the presence of air [53]. On contrary, Zapata et al used different method for silane treatment where objective was to impart hydrophobic properties to zeolite [41]. Organo-silane groups with different alkyl lengths were adsorbed on surface using liquid phase method where zeolite sample was first dissolved in solvent, followed by the addition of silane compound under stirring condition at room temperature. Sample was recovered by filtrations and washed with ethanol [41]. Main difference between two methods were formation of silane compounds on the surface of zeolites. Formation of  $\text{SiO}_2$  units on surface was mainly used to achieve selective adsorption and reduce coke formation. HMCM-22 was modified with tetraethoxysilane (TEOS) for selective skeletal isomerization of n-butene to isobutene [54].

H-USY was functionalized by octadecyltrichlorosilane (OTS) where silane compounds with their organic part attached with surface to make it hydrophobic, in the application of bio fuel upgrading [41] . Table 7 gives the overview of silane treated zeolites and their applications.

**Table 7. Silane treated zeolites and their application.**

<b>Zeolite</b>	<b>Silane groups</b>	<b>Application</b>	<b>References</b>
MCM_41	dimethoxydimethylsilane (DMODMS) and dichloromethylphenylsilane (DCMPS)	competitive adsorption of water and toluene	[55]
H-USY	Octadecyltrichlorosilane (OTS), hexyltrichlorosilane (HTS), and ethyletrichlorosilane.	Bio fuel upgrading.	[39]
MCM-22	dichlorodimethylsilane (DCDMS)	To improve thermal stability of silylated zeolite.	[56]
HY	octadecyltrichlorosilane (OTS)	Bio fuel upgrading in hot aqua environment.	[41]

HMCM-22	Tetraethoxysilane (TEOS), silicon tetrachloride (SiCl <sub>4</sub> ) and 8-hydroxyquinoline	selective skeletal isomerization of n- butene to isobutene	[57]
ZSM-5	TEOS	shape selectivity	[54]

## 2.8 Objective

1. Steam-assisted catalytic cracking of heavy oil over surface modified zeolite catalyst to increase the production of lighter hydrocarbons.
2. Surface modification of catalysts using organosilane compound through two techniques i.e. vapor phase deposition and liquid phase deposition
3. Improve the hydrophobicity and stability of catalysts.

## CHAPTER 3

### Methodology and Experimental

#### 3.1 Surface modification of catalyst using silane compound

Beta zeolite catalyst (BEA) with  $\text{SiO}_2/\text{Al}_2\text{O}_3$  150 was provided by Catalysis Society of Japan. Firstly, BEA catalyst was ion exchanged using convention method [58, 59], typically, 1 g of catalyst was suspended in 20 g of 2 M ammonium nitrate ( $\text{NH}_4(\text{NO}_3)$ ) solution and the solution was heated under stirring for 3 h. Final solution was centrifuge to remove ( $\text{NH}_4(\text{NO}_3)$ ) solution from catalyst. This procedure was repeated thrice. Finally  $\text{NH}_4^+$ -BEA zeolite was dried at 100 °C for 12 h.  $\text{NH}_4^+$ -BEA was first pelletized to get ca. 0.3 mm in diameter pellets and then calcined at 550 °C for 3h in an air stream. After calcination H-BEA was used as BEA-parent catalyst in cracking reactions. While for BEA-silane treated samples, pelletized  $\text{NH}_4^+$ -BEA were used directly in silane treatment.

#### 3.2 Vapor phase silane treatment

Tri phenyl silane was used as a silane reagent.  $\text{NH}_4^+$ -BEA pellets in a packed bed reactor were first air calcined at 550 °C, then H-BEA zeolite was exposed to vapor of tri phenyl silane at 373-393 K in a  $\text{N}_2$  stream. After 1 h feed of silane was stopped to remove the physically adsorb silane compounds on surface. Zeolite brought in the contact with silane compound vapor twice [53]. Finally modified catalyst was used as BEA-silane treated catalyst in heavy oil cracking reaction.

### 3.3 Liquid phase silane treatment

H-BEA zeolite was modified in liquid phase using procedure described by Zapata et al [41]. As a typical run 1 g of zeolite was dispersed in 20 ml of toluene and sonicated for 20 mins at room temperature. Triphenyl silane (0.5mmol/g zeolite) was added in zeolite/toluene mixture and stirred for 24 h at room temperature. Finally, zeolite was collected by filtration and washed several time with ethanol. Modified zeolite was then dried at 100 °C overnight.

### 3.4 Steam assisted catalytic cracking of heavy oil

Fixed-bed type reactor was used for cracking of atmospheric residue (AR) with steam at a reaction temperature of 470 °C and a pressure of 1 atm for 2 and 4 h. Reactor setup is shown in Figure. 10. AR was diluted with toluene to 10% to reduce its viscosity. Toluene inactivity with catalysts were confirmed in previous study elsewhere [60]. Nitrogen, steam and feed mixture were fed to the reactor simultaneously with the flow rate of 5 mL/min, 5 mL/h and 2.9 mL/h, respectively. The W/F was 4 h, where W was the weight of catalyst (g), F was feed flow rate ( $\text{g}\cdot\text{h}^{-1}$ ),  $F_{\text{H}_2\text{O}}/F$  was 2 ( $F_{\text{H}_2\text{O}}$ : water flow rate/  $\text{g}\cdot\text{h}^{-1}$ ). The water injection line was heated to 160 °C to convert water into superheated steam. Previously, all reaction conditions were optimized to get maximum conversion. The liquid and gaseous products were collected with condenser and gas bag respectively. A quantitative gas product analysis was made using gas chromatography, which was equipped with a thermal conductivity detector (TCD; model GC-8A, Shimadzu, Ltd), a flame ionization detector (FID; model GC-12A, Shimadzu, Ltd), activated carbon and Porapak-Q columns, respectively. The liquid products were analyzed using high

performance liquid chromatograph (model: CTO-10A, Shimadzu, Ltd). Carbon number  $<C_6$  was not included in production yield. Toluene detected was also excluded in the calculations. The mass balance error was  $<5\%$  in preliminary experiments using AR as feedstock without solvent [60-62].

1 g of catalyst was loaded in reactor along with cotton wool on the top and bottom to support the catalyst bed. 0.02 g of cotton wool, 2 g of marble beads, 1g catalyst and 0.02 g cotton wool were loaded in sequence. Steam input line was wrapped with tap heater to maintained the temperature at  $160\text{ }^{\circ}\text{C}$ . Both steam and feed were injected in the reactor simultaneously. Reactor temperature was maintained at  $470\text{ }^{\circ}\text{C}$  through electrical heater. Outlet temperature of reactor was maintained at  $100\text{ }^{\circ}\text{C}$ . Steam injection continued for 0.5 h after reaction to remove left products from reactor.

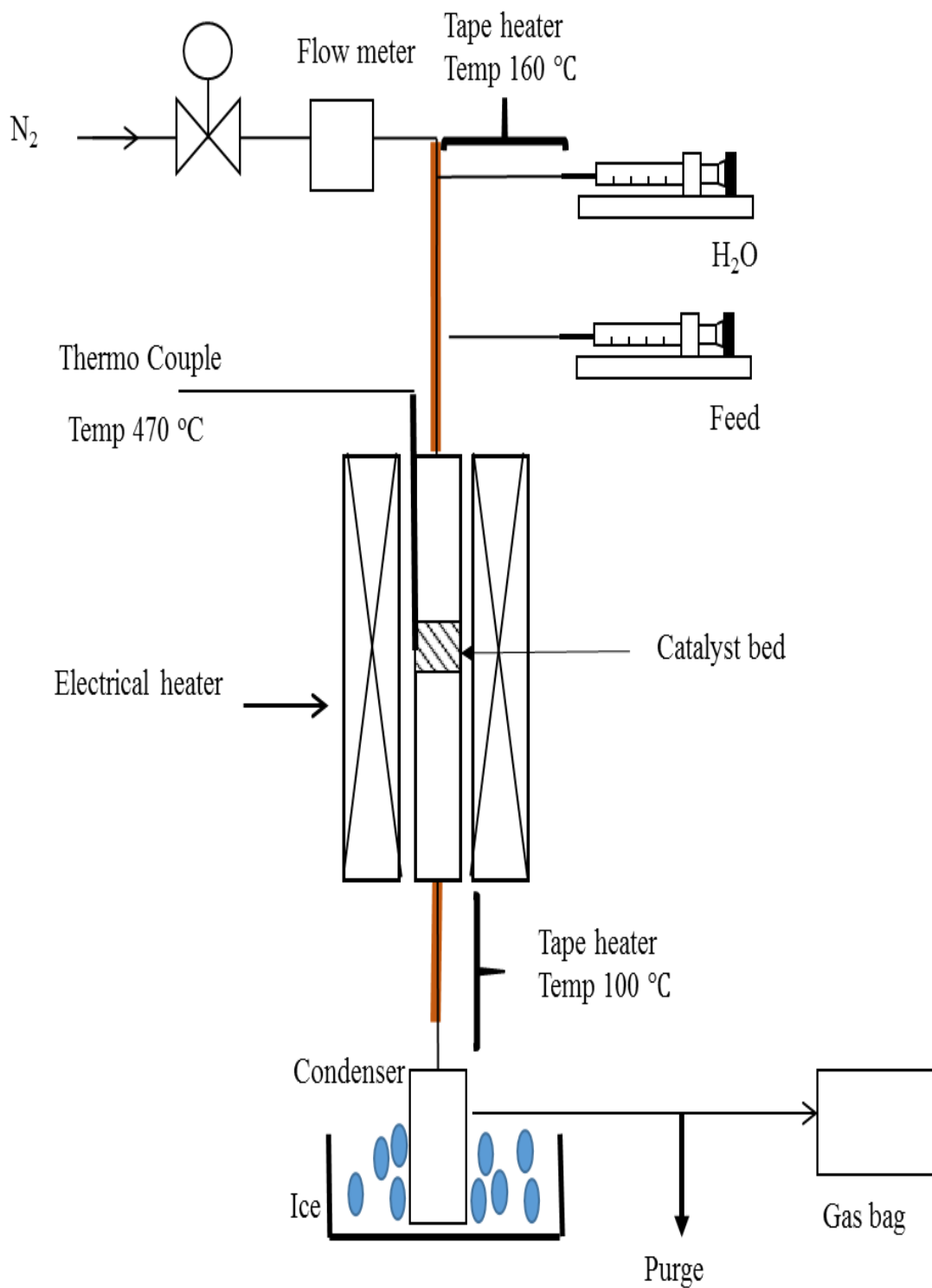


Figure 10. Experimental setup of fixed-bed flow reactor.

### 3.5 Characterization of catalysts

All BEA zeolite catalysts structure and phase purity was confirmed by using X-ray diffractometer (Ultima IV, Rigaku). Texture properties of catalysts were obtained using an N<sub>2</sub> adsorption isotherm (Belsorp mini, BEL Japan). Acidity was measured using NH<sub>3</sub>-TPD method. A 1.0% NH<sub>3</sub> was used as carrier gas at 273-550 °C temperature range and 5 °C.min<sup>-1</sup> heating rate was maintained. To establish measurement under complete adsorption equilibrium conditions, NH<sub>3</sub> molecules desorption from acid sites of zeolite was performed under a 1.0% NH<sub>3</sub>-He atmosphere [63]. Brønsted acid sites (BAS) and Lewis acid sites (LAS) were measured using Fourier transform infrared (FT-IR) equipped with pyridine adsorption support. Diffuse reflectance infrared Fourier transform (DRIFT) spectrometer with mercury cadmium telluride (MCT) detector (FT/IR-4100, JASCO) was used. A total of 200 Scans were averaged for each spectrum. Sample was pre-treated in vacuum at 500 °C for 12 h and then pyridine was adsorbed onto the sample at 100 °C for 2h. Nitrogen was introduced to remove physically adsorbed pyridine at 100 °C for 0.5 h. Lastly, sample acidity was measured via FT-IR analysis at 100 °C [64].

## CHAPTER 4

### Vapor phase silane treated catalysts

Steam assisted catalytic cracking of AR over Beta zeolite catalyst were studied. To enhance the yield of lighter components, BEA zeolite surface was modified using triphenyl silane and catalysts were tested in AR reaction at two different reaction times i.e., 2 h and 4 h. Organo-silane compound was selected on the basis of its kinetic diameter, which should be larger than the pore size diameter of BEA catalyst so that silane compound only modify the external surface of catalyst [41]. As described earlier, vapor phase silane treatment method was employed to modify the catalysts. Protonated BEA catalysts were silane treated and used in the reaction. The cracking products were classified according to their carbon number into six groups: gas, Gasoline + kerosene (C<sub>7</sub>-C<sub>13</sub>), Gas oil (C<sub>14</sub>-C<sub>20</sub>, C<sub>21</sub>-C<sub>35</sub>), and heavy oil (C<sub>36</sub>-C<sub>44</sub>, above C<sub>45</sub>).

## 4.1 Effect of silane treatment on catalysts properties

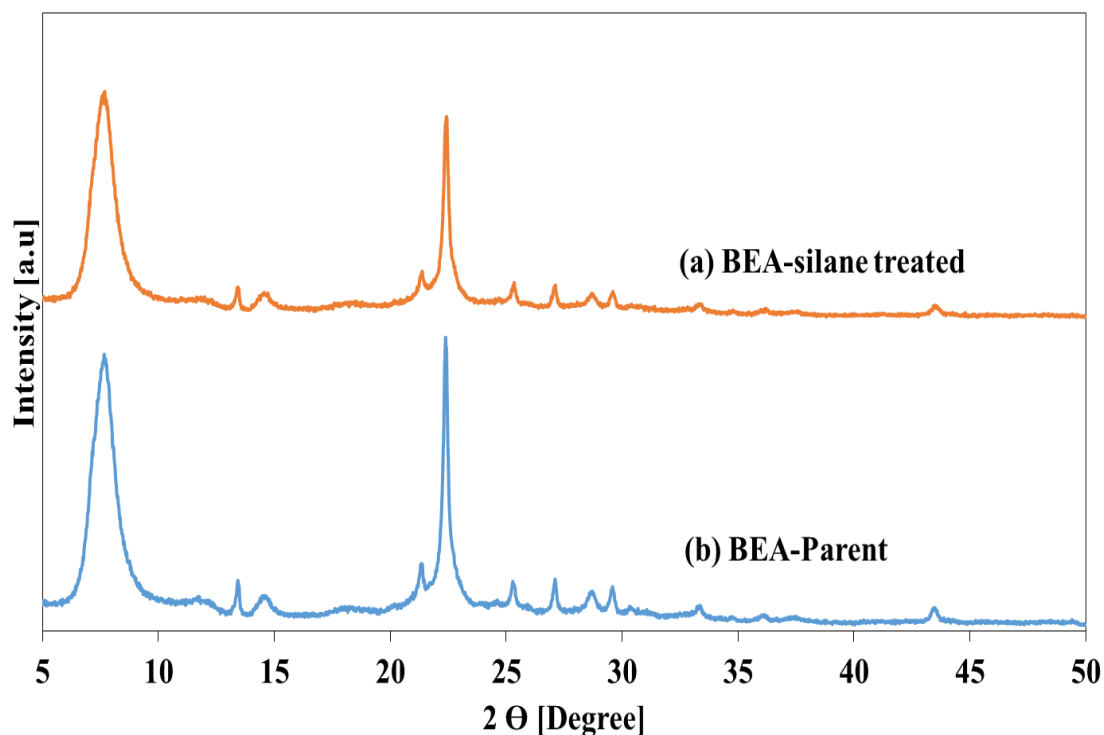


Figure 11. XRD patterns of (a) BEA-Silane treated and (b) BEA-Parent.

Figure. 11 shows the comparison of two XRD patterns: BEA-parent and BEA-silane treated catalysts, which clearly indicates that after silane treatment, catalyst retained its crystallinity and structure. It is important to measure the effect of silane treatment on the acidity and the activity of BEA catalyst. After surface modification, it was expected that the acidity of the catalysts was reduced. This statement is supported by  $\text{NH}_3$ -TPD results as shown in Figure. 14  $\text{NH}_3$ -desorption peak, which is associated with strong acid sites (above 580 K) showed a decline for BEA-silane treated zeolite.

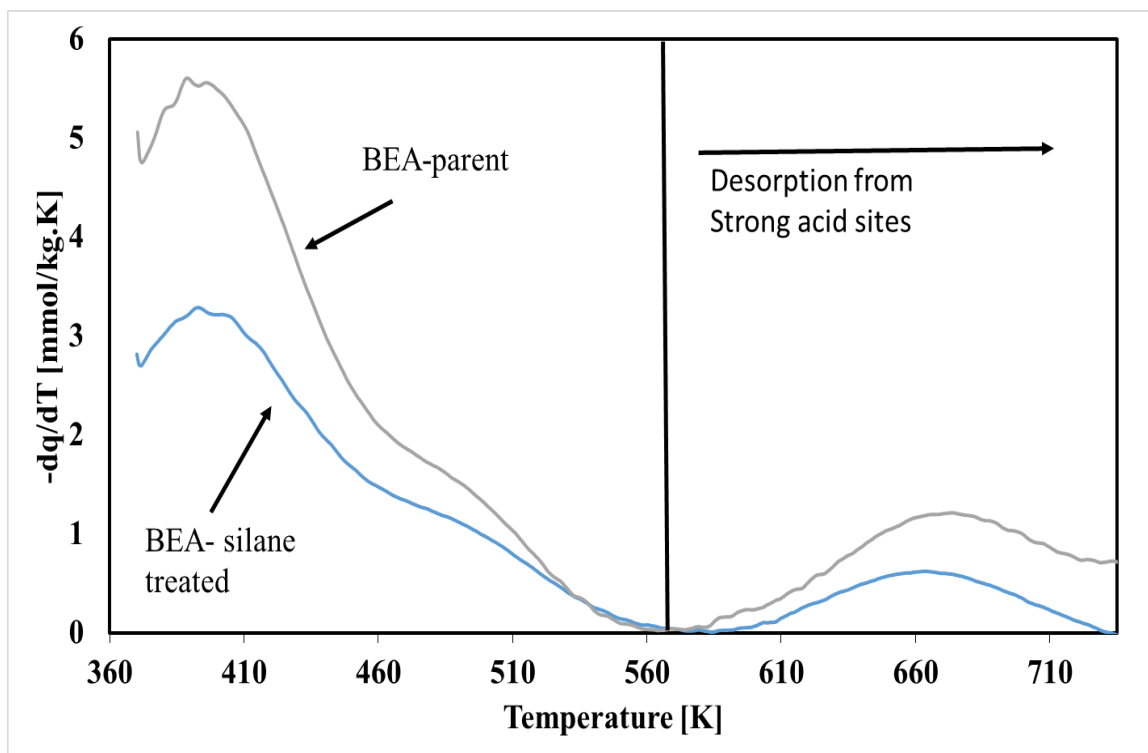


Figure 12. NH<sub>3</sub>-TPD profiles of BEA-Parent and BEA-silane treated zeolite catalysts.

Previous research on catalytic cracking of alkanes over zeolites already proved the role of strong acid sites, where high acidity provides more sites for cracking but at the same time leads to more coke formation and hence fasten the deactivation of catalysts [65, 66]. In order to take a deeper look into the change in acidity of silane treated catalyst, Brønsted acid sites (BAS) and lewis acid sites (LAS) were measured qualitatively using FT-IR pyridine. The IR spectra in Figure.13 show full agreement with NH<sub>3</sub>-TPD results. Decrease in both BAS (1540 cm<sup>-1</sup>) and LAS (1460 cm<sup>-1</sup>) were observed after silane treatment. Roles of BAS in cracking reactions were discussed by many researchers [67, 68] but it is also worth mentioning that hydrophilicity of catalysts are also associated with BAS [41, 69]. Hence, the role of BAS in steaming environment during cracking reaction has significant importance. Silane treatment procedure did not include post calcination step unlike catalytic cracking of silane (CCS) in which SiO<sub>2</sub> units were formed on active

sites after calcination [52, 53, 64]. It was expected organic groups of organo-silane compounds attached on outer surface and prohibited the attack of water (steam) molecules on surface [41]. N<sub>2</sub> adsorption analysis supported the concept of outer surface modification of catalyst as only outer surface area measured using t-plot method was increased as shown in Table 8. Moreover, small increase in micropore volume was observed in Figure. 14.

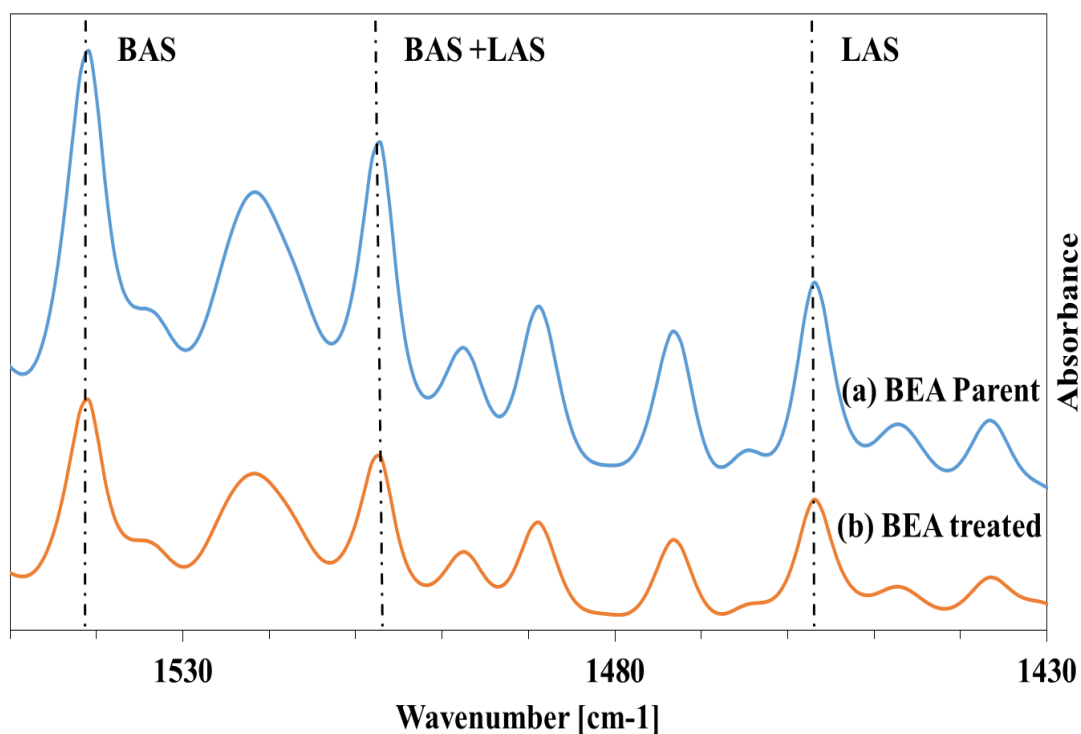


Figure 13. FT-IR spectra of pyridine-adsorbed (a) BEA-Parent and (b) BEA-Silane treated zeolite catalysts.

Table 8. Textural properties of parent and modified BEA catalyst using vapor silane treatment.

Samples	$S_{\text{BET}}^{\frac{2}{-1}}$ [m g ]	$S_{\text{EXT}}^{\frac{2}{-1}}$ [m g ]	$V_{\text{micro}}^{\frac{3}{-1}}$ [cm g ]
BEA- Unmodified	422	62	0.1614

$S_{\text{BET}}$  : surface area by BET method;

$S_{\text{EXT}}$  and  $V_{\text{micro}}$  : external surface area and micro pore volume by t-plot method.

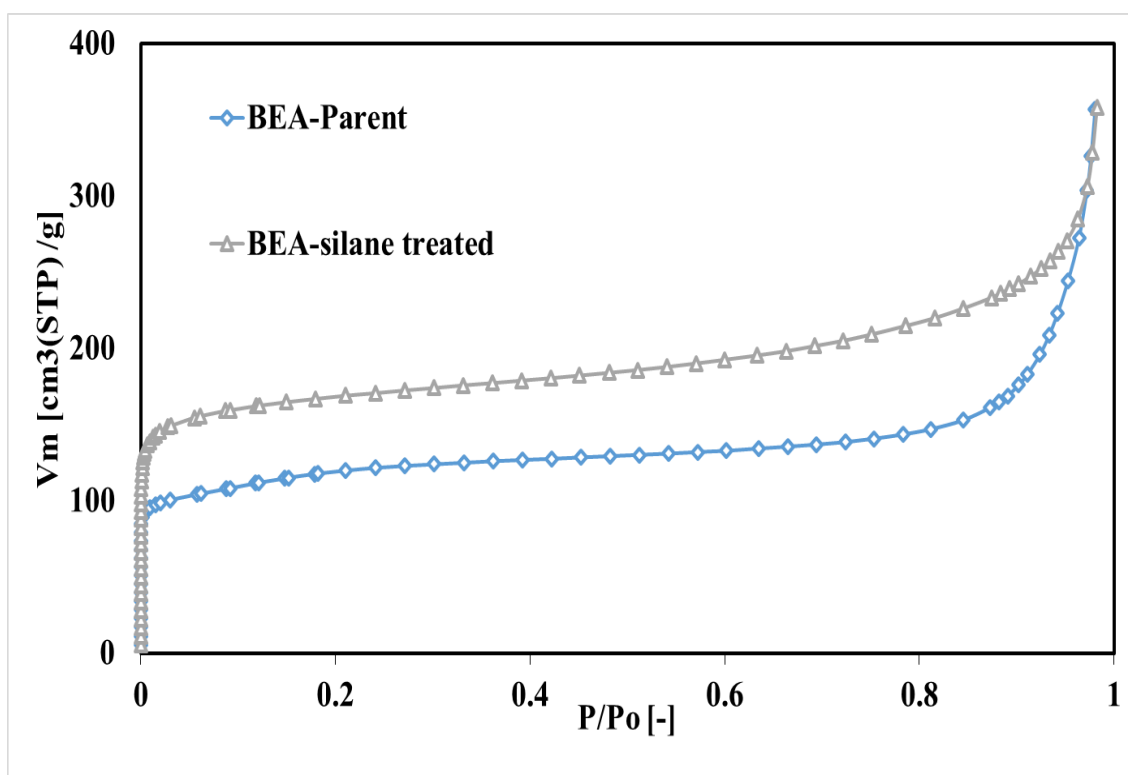


Figure 14. N<sub>2</sub> adsorption isotherms of BEA-Parent and BEA-Silane treated.

## 4.2 Effect of surface modified catalyst on cracking of AR

Steam dilutes the reaction mixture and thus decreases the amount of coke formation [70], but irreversible deactivation (dealumination) of zeolite catalysts is a major problem in the presence of steam [71]. Numerous previous research papers showed a decrease in the dealumination process under steam environment after the incorporation of promoters such as phosphorus, lanthanum, cerium and fluorides [44, 46, 72, 73]. Moreover, other than these problems, zeolite structural changes were also reported in an aqueous

environment [39, 41]. Silane treatment of zeolite catalyst, developed in this work, mitigated the effects of dealumination, coking and structural changes. As shown in Figure. 15, 55.7 mol% of gasoline and kerosene ( $C_7-C_{13}$ ) were produced over the BEA-silane treated catalyst, which was significantly higher than the 30.9 mol % of same carbon numbers over BEA parent catalyst for reaction time of 2 h. The total yield of lighter component ( $C_7-C_{35}$ ) over BEA-silane treated catalyst was 59.4 mol%. Yield of lighter component were higher than the ones obtained over metal oxide catalysts used previously in the presence of steam [60-62]. It should be noted that BEA-silane treated catalyst produced negligible amount of heavy hydrocarbon ( $C_{20+}$ ) as compared to BEA-parent catalyst (26.7 mol% heavy hydrocarbon). Amount of coke formed after 2 h reaction over BEA-silane treated catalyst was 6 wt. % of catalyst as compared to 11.5 wt. % over BEA-parent catalyst. This indicates the formations of heavier hydrocarbons were suppressed in accordance with the surface properties of BEA- catalyst. No hydrogen was formed in the case of both parent and silane treated zeolites as shown in gas composition analysis (Figure. 16), while hydrogen was the main constituent in heavy oil reactions over metal oxides catalysts. This fact also verified the reduction of coke formation in BEA-zeolite catalysts. As it has been shown in many previous reports that zeolite catalysts were preferred over many other type of catalysts for their high tendency of producing olefins and paraffin [70, 71]. This statement was supported with gas composition analysis in Figure. 18 where mainly alkenes and alkanes were formed and no  $CO_2$  evolved which mainly formed in oxidative cracking reactions over iron-oxide catalysts [62].

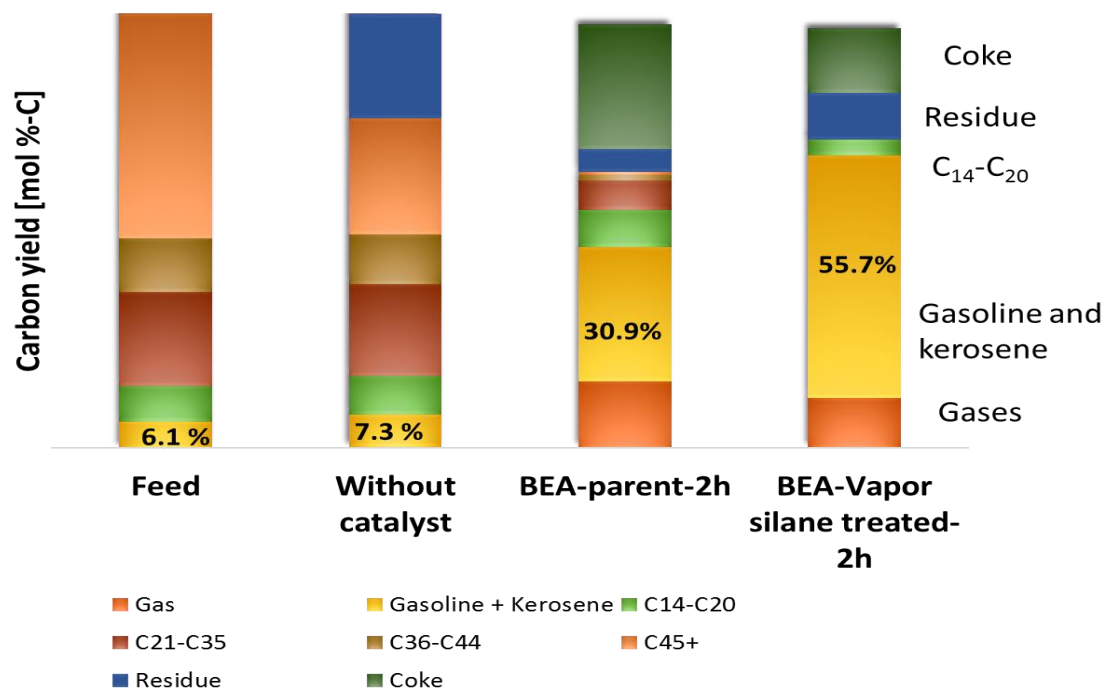


Figure 15. Carbon yield after 2 h reaction of AR with steam over BEA-parent and BEA-silane treated catalysts.

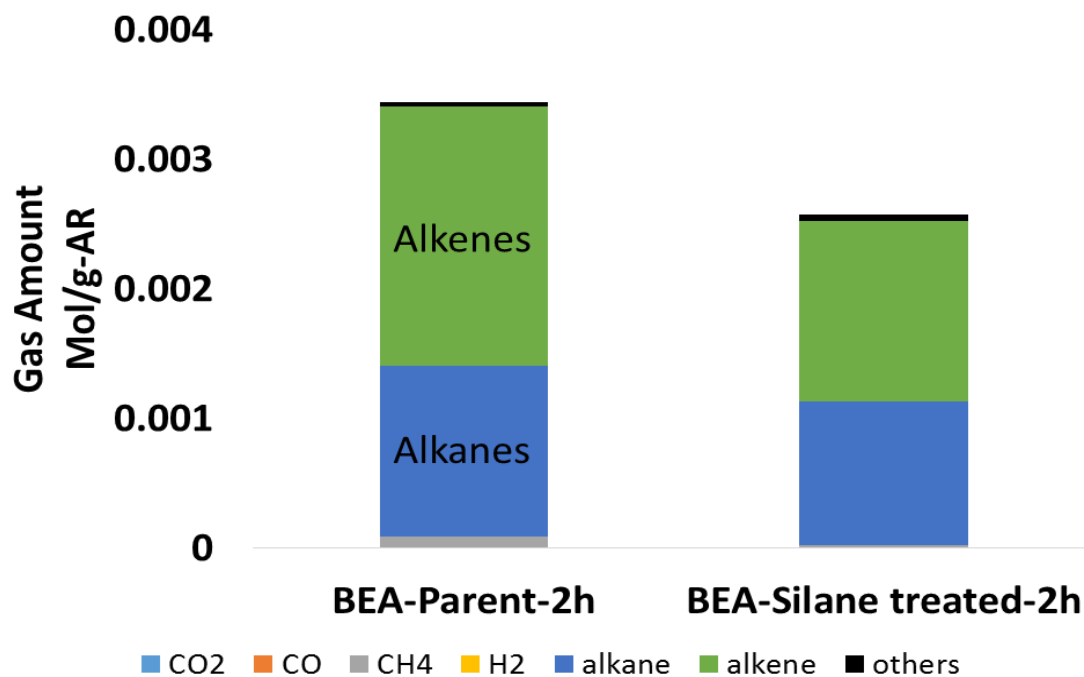


Figure 16. Gas composition (mol/g-AR) after 2 h reaction of AR with steam over BEA-parent and BEA-silane treated catalysts.

Better view on liquid hydrocarbon molecular weight (MW) distribution is presented in Figure. 17. Higher peak of liquid product curve for silane treated BEA catalyst in lower hydrocarbon MW range (less than 200 g/mol) shows considerable amount of lighter component yields. Figure. 18 shows a physical appearance of liquid product obtained after 2 h reaction time. Light green color of liquid product produced over silane-treated BEA catalyst suggests qualitatively the presence of a higher yield of lighter component as compared to BEA-parent catalyst.

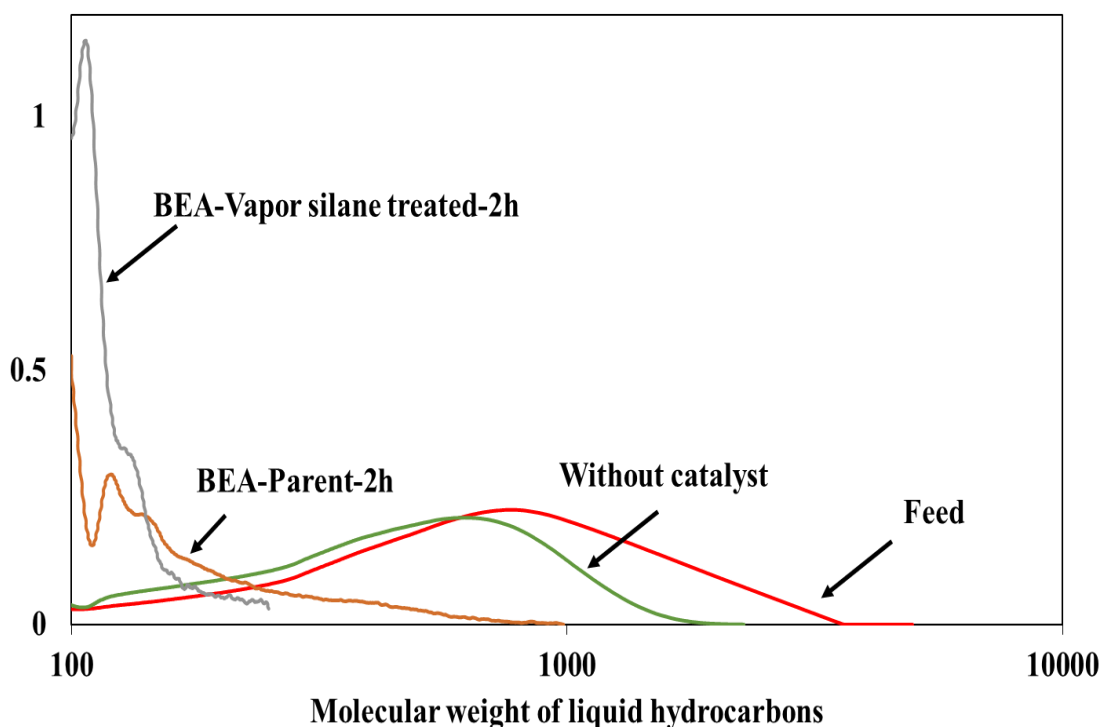


Figure 17. Molecular weight distribution of liquid product after 2 h reaction time.



**Figure 18. Physical appearance of liquid product after 2 h reaction time over (a) BEA-parent and (b) BEA-silane treated catalysts.**

Structural changes after the 2 h reaction time were observed in  $N_2$ -adsorption isotherms as shown in Figure. 19. Prior to  $N_2$  adsorption studies, the spent BEA-parent and BEA-silane treated catalysts were calcined. BEA-parent catalyst showed an increase in surface area which may ascribe to the dealumination during steam-assisted reaction. In contrary, BEA-silane treated catalyst was found to be resistant to the attack of steam. The surface

organo-silane compounds prevented dealumination, which usually occurred under steam environment as shown in Figure. 20, N<sub>2</sub>-adsorption isotherms of both BEA-silane treated catalyst before and after reaction shows exactly the same trends. Figure. 21 shows the comparison of XRD patterns for parent and silane treated catalysts. Both samples retained their crystallinity after 2 h reaction under steam exposure. Moreover, no impure phase was observed. This concludes that even though after the 2 h exposure to steam, the BEA catalyst structure was stable.

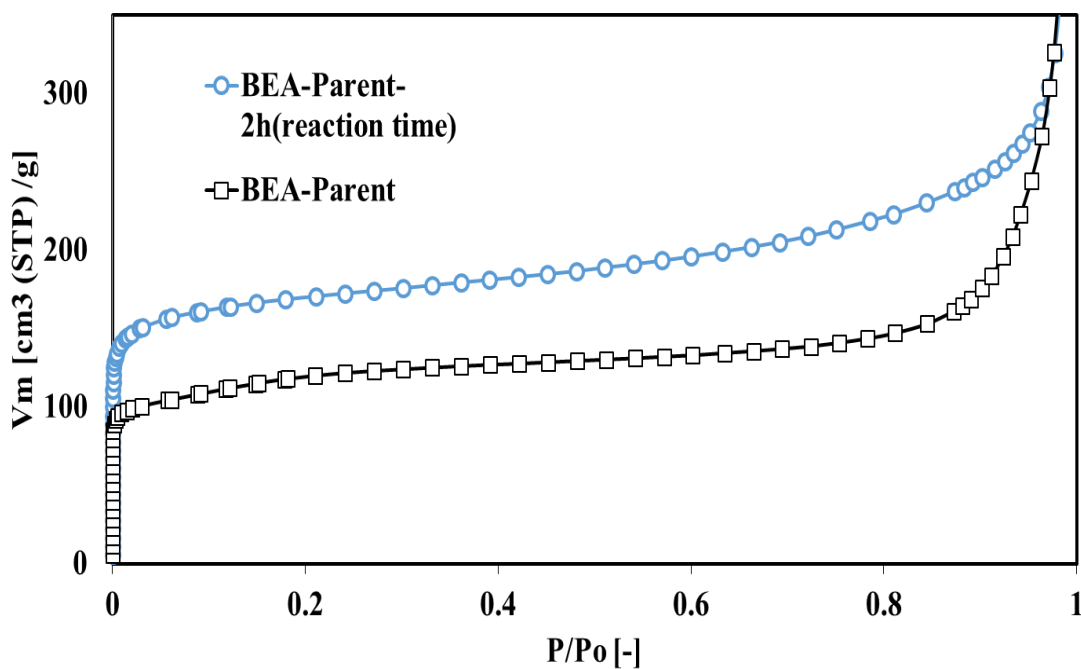


Figure 19. N<sub>2</sub> adsorption isotherms of spent BEA-Parent-2h (after recalcination) and BEA-parent.

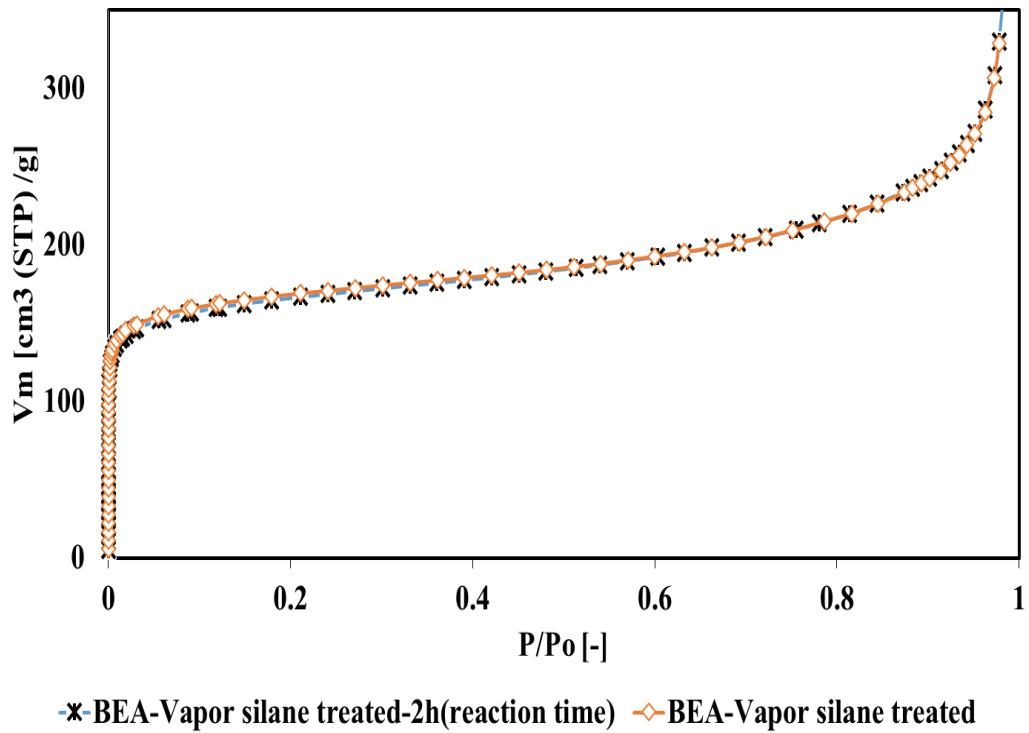


Figure 20. N<sub>2</sub> adsorption isotherms of spent BEA-silane treated-2h(after recalcination) and BEA-silane treated

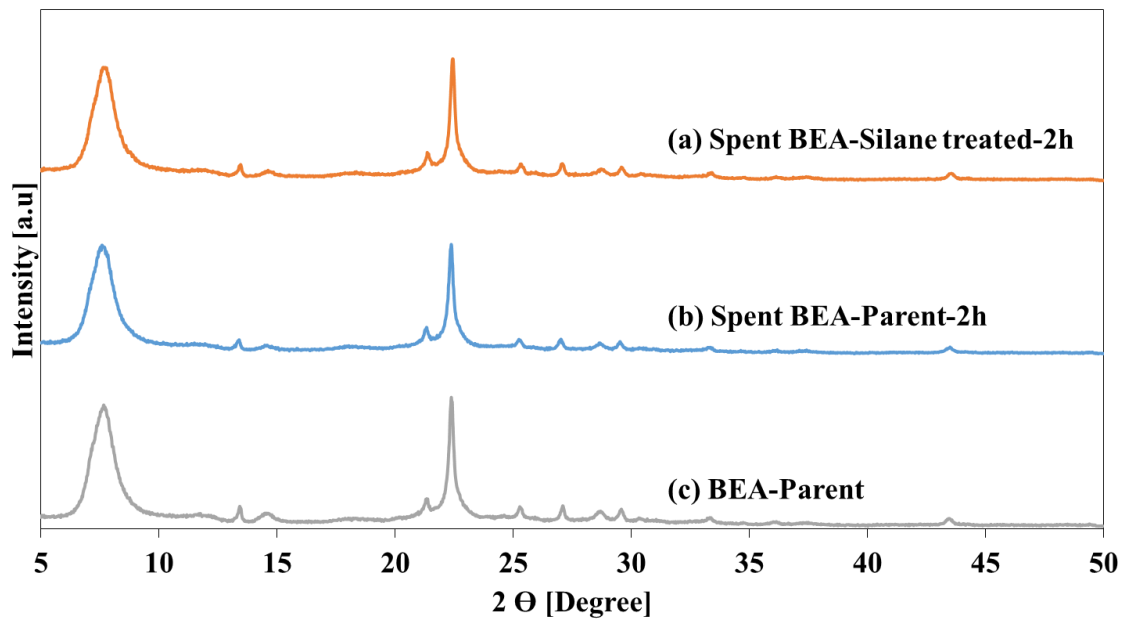


Figure 21. XRD patterns (a) BEA-silane treated-2h (b) BEA-parent-2h (c) BEA-Parent.

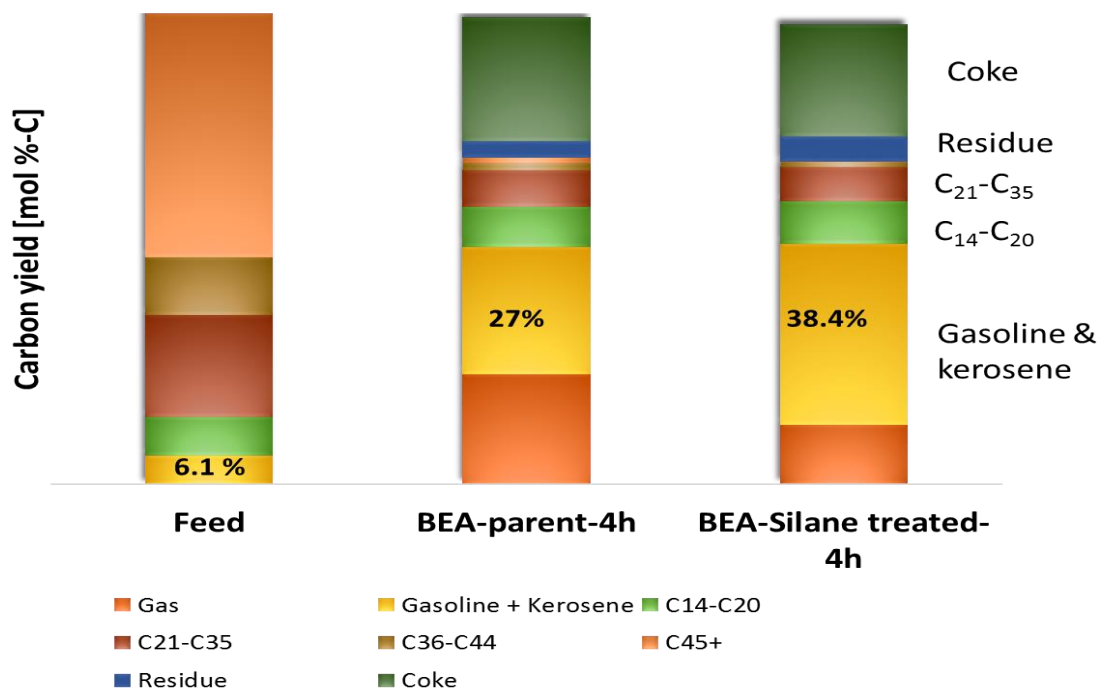


Figure 22. Carbon yield after 4 h reaction of AR with steam over BEA-parent and BEA-silane treated catalysts.

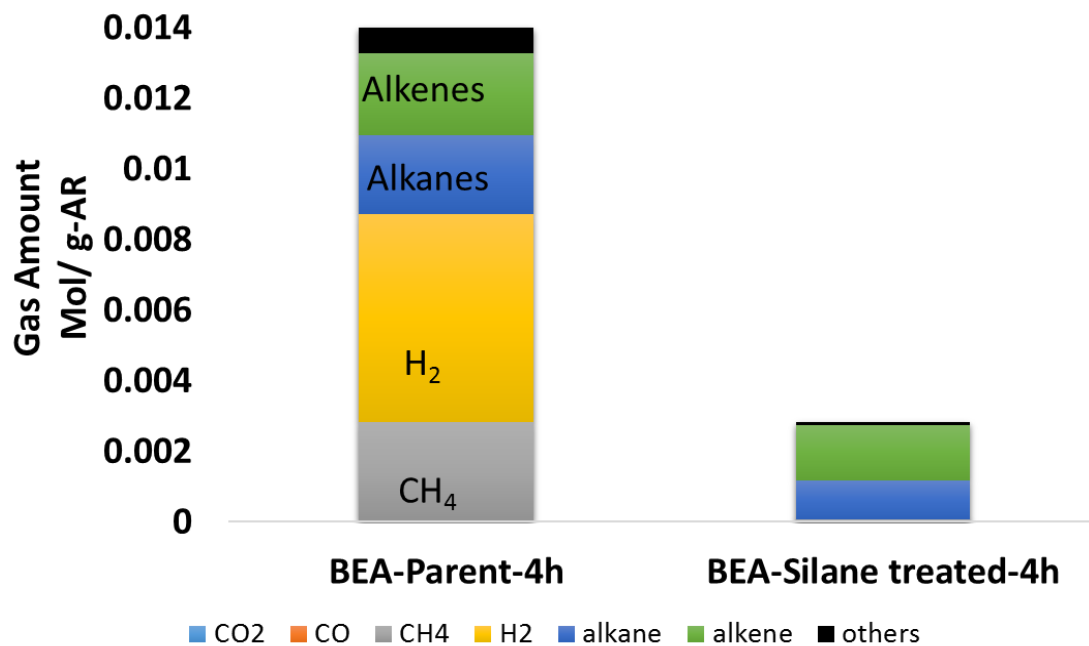


Figure 23. Gas composition (mol/g-AR) after 4 h reaction of AR with steam over BEA-parent and BEA-silane treated catalysts.

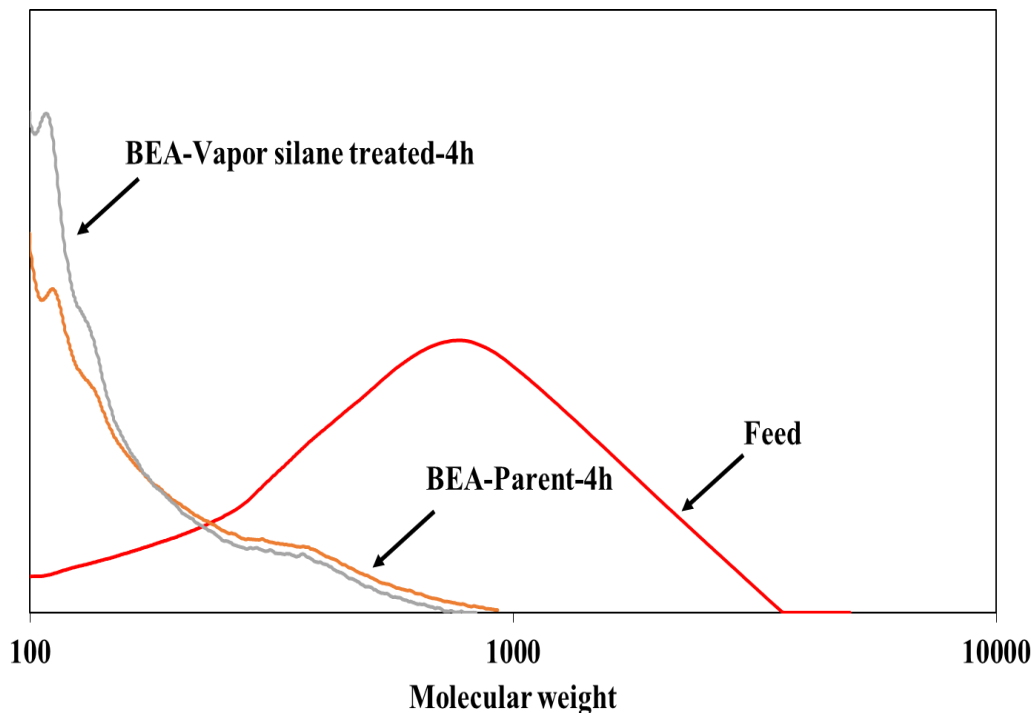


Figure 24. Molecular weight distribution of liquid product after 4 h reaction time.

### 4.3 Effect of reaction time on the stability of parent and modified catalyst

To investigate the stability of BEA-parent and BEA-silane treated catalysts, reaction time was increased to 4 h and the same sequence of reactions were performed. Product distribution (mol %) was also reported to study the effect of time. It was observed in Figure. 22 that lighter component yield after 4 h reaction decreased for both parent and silane treated zeolites as compared to 2 h reaction time; this finding is obvious as the amount of coke increased with time. Regardless of reaction time, percentage increase in lighter component yield was approximately same after silane treatment. Gas composition analysis in Figure. 23 shows a larger concentration of gas produced (mol per g-AR) over

BEA-parent, in addition mainly hydrogen evolved, which indicates the coke formation. Hydrocarbon MW distribution curves in Figure. 24 shows lighter products were formed over BEA-silane treated zeolite after 4 h reaction. Physical appearance of liquid product after 4 h reaction time in Figure. 25 justifies the results of MW distribution trends. Light yellow color of liquid product over BEA-silane treated zeolite after 4 h indicates the presence of lighter ends. Same color was observed after 2 h reaction over BEA-parent catalyst (Figure. 25).



**Figure 25. Physical appearance of liquid product after 4 h reaction time over (a) BEA-parent and (b) BEA-silane treated catalysts.**

Change in the phase purity of BEA-parent after 4 h reaction time was studied using XRD analysis. XRD patterns in Figure. 26 shows that an impure phase appears in BEA-parent catalyst, while BEA-silane treated catalyst retained its crystallinity and purity. Two peaks at  $9 [2 \Theta^\circ]$  and  $24 [2 \Theta^\circ]$  indicates that BEA-parent catalyst loses its purity during 4 h continues exposure to steam at 743 K

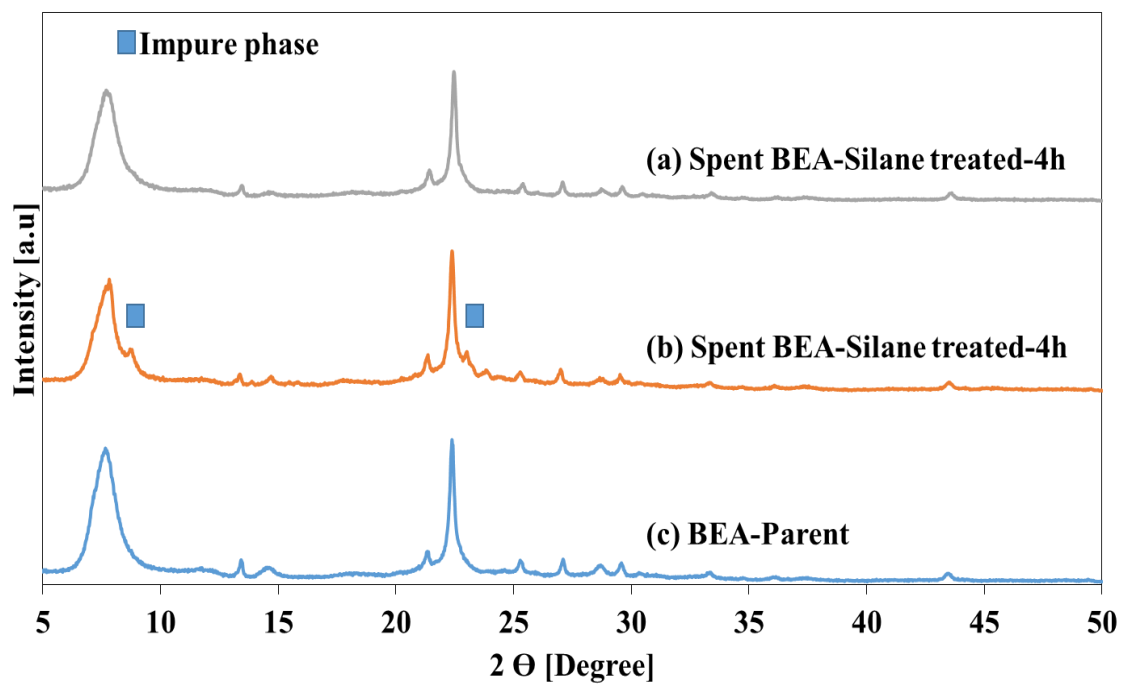


Figure 26. XRD patterns of (a) spent BEA-silane treated-4h (b) spent BEA-parent-4h (c) BEA-parent.

## CHAPTER 5

### Liquid phase silane treated catalysts

#### 5.1 Effect of silane treatment on catalyst properties

Liquid phase deposition of silane compound on BEA zeolite ( $\text{SiO}_2/\text{Al}_2\text{O}_3 = 150$ ) was adapted following a procedure reported earlier by Zapata et al [39]. Triphenyl silane as a reagent was selected on the basis of its kinetic diameter, which should be larger than the pore size of BEA. Figure. 27 shows the XRD patterns of parent BEA and liquid phase silane treated BEA zeolites. No change in purity of phase was observed, while a very less change in crystallinity was noted as expected after the surface modification of zeolite.  $\text{N}_2$ -adsorption isotherms in Figure. 28 shows that adsorption over both parent and silane treated catalysts are approximately same. Table 9 presents the change in detailed texture properties after modification which again shows the increase in external surface area, attributes that organosilane compounds attached to the only external surface of BEA catalysts and did not enter into the pore of BEA zeolite. These findings were important because the inner acidity of zeolite remained unaltered and available for cracking reactions. Figure. 29 shows the  $\text{NH}_3$ -TPD profiles of parent and silane treated zeolites. A decrease in both weak and strong acid sites was observed.  $\text{NH}_3$  desorption peak at temperature above 600 K associated with strong acid sites showed a decrease trend after modification. Silane compounds attached to both weak and strong sites, which were located at the outer surface of Beta zeolite. Large number of acid sites increases the activity of catalyst and provides more sites for cracking reaction. However, it was also

found that the coke formation linearly increases with activity of catalyst. Hence, silane groups attached to the selective acid sites also controls coke formation [65, 66].

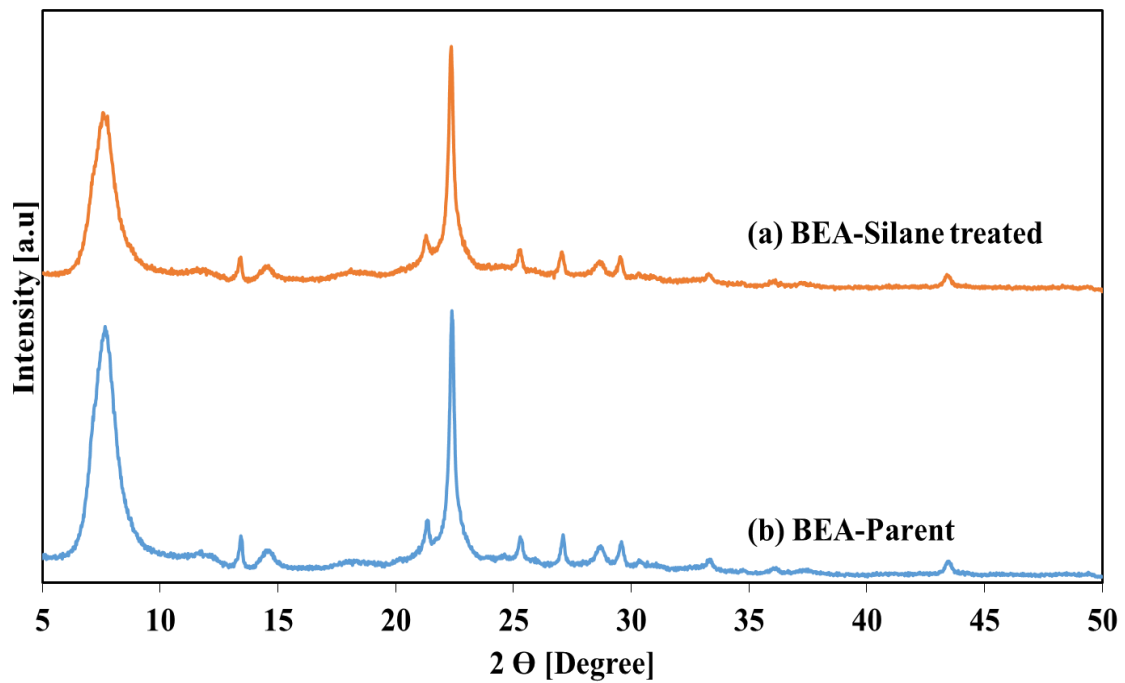


Figure 27. XRD patterns of (a) BEA- Liquid Silane treated and (b) BEA-Parent.

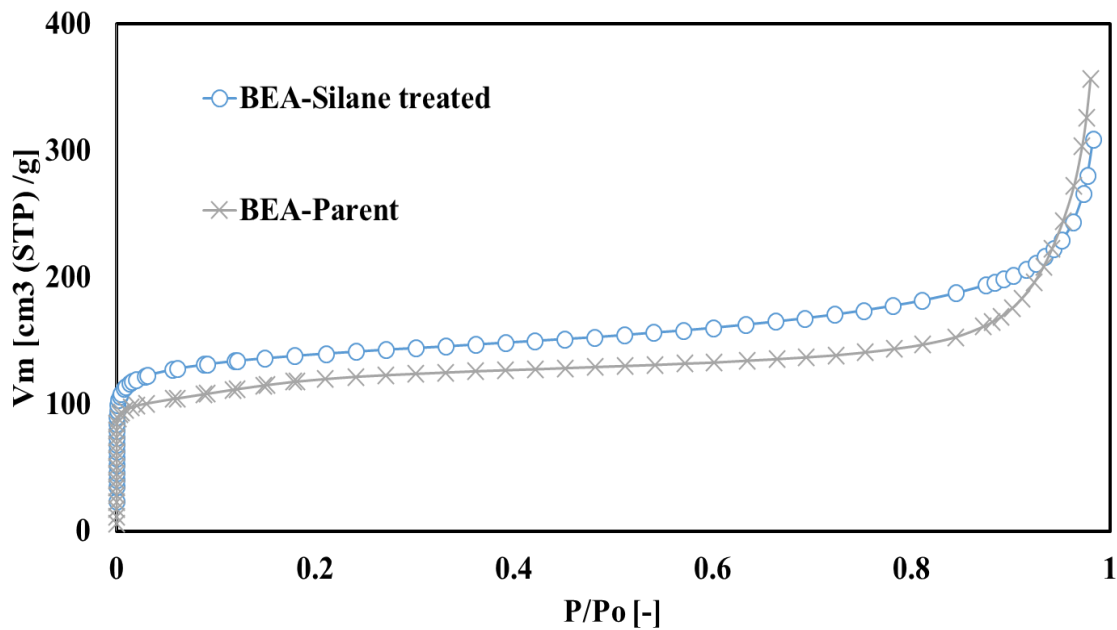


Figure 28. N<sub>2</sub> adsorption isotherms of BEA-Parent and BEA-Liquid silane treated.

Table 9. Textural properties of parent and silane treated BEA catalysts.

Samples	$S_{\text{BET}}^{\text{2}^{-1}}$ [m <sup>2</sup> g <sup>-1</sup> ]	$S_{\text{EXT}}^{\text{2}^{-1}}$ [m <sup>2</sup> g <sup>-1</sup> ]	$V_{\text{micro}}^{\text{3}^{-1}}$ [cm <sup>3</sup> g <sup>-1</sup> ]
BEA-Parent	422	62	0.1614
BEA-Silane Treated	415	114	0.1652

$S_{\text{BET}}$  : surface area by BET method;

$S_{\text{EXT}}$  and  $V_{\text{micro}}$  : external surface area and micro pore volume by t-plot method.

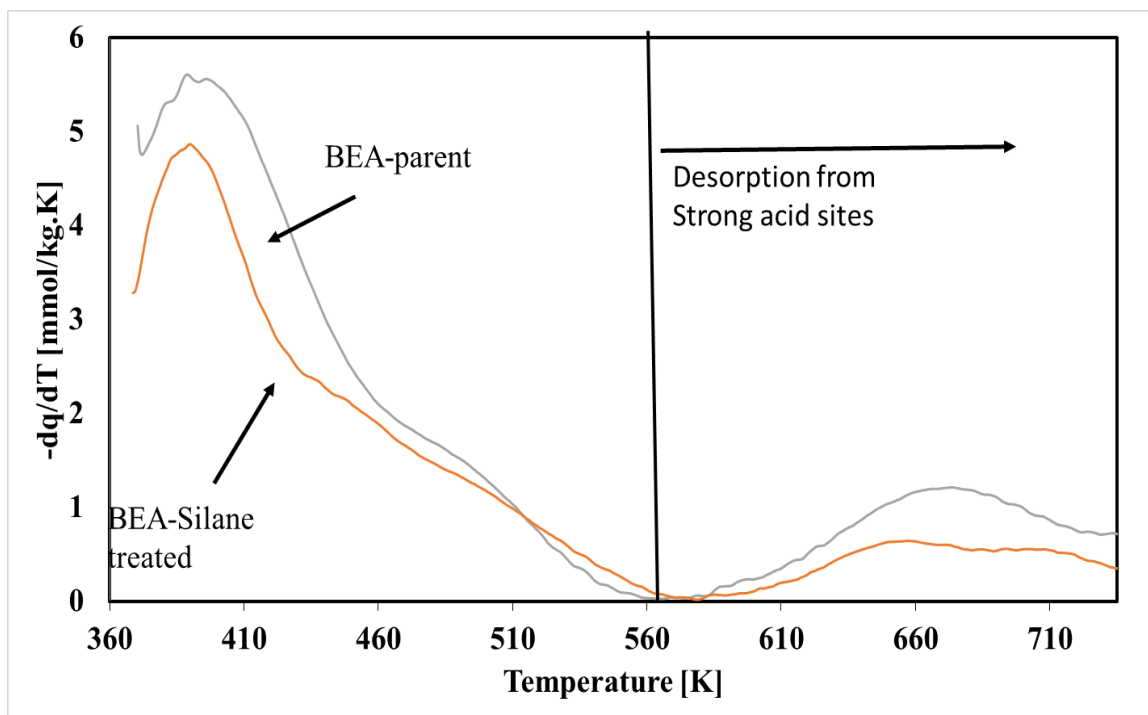


Figure 29. NH<sub>3</sub>-TPD profiles of BEA-Parent and BEA-Liquid-silane treated zeolite catalysts.

## 5.2 Effect of surface modified catalyst on cracking of AR

Surface modified BEA zeolite was tested in heavy oil cracking reaction for 2 h and 4 h reaction time. The products were classified according to their carbon number into six groups: gases, gasoline + kerosene (C<sub>7</sub>-C<sub>13</sub>), gas oil (C<sub>14</sub>-C<sub>20</sub>, C<sub>21</sub>-C<sub>35</sub>), and heavy oil (C<sub>36</sub>-C<sub>44</sub>, above C<sub>45</sub>). To investigate the effect of surface modification on the cracking of atmospheric residue oil, silane treated catalyst was evaluated for 2 h reaction time and liquid as well as gas product distribution was analyzed. Steam plays important role in the cracking reactions over zeolite catalysts as it helps to decrease the amount of coke formation but at the same time dealumination of zeolite catalyst in the presence of steam is a major problem [47, 70, 74]. Reducing the rate of dealumination using silane treated zeolite tends to increase conversion of heavy feedstock into lighter hydrocarbon. This

assumption is verified in Figure. 30 which represent the increase in gasoline ( $C_7-C_{13}$ ) yield over silane treated BEA zeolite catalyst as compared to the parent BEA catalyst. Also the yield of lighter hydrocarbon products ( $C_7-C_{35}$ ) increased up to 50.3 mol%. These results indicate that silane treated BEA catalyst retained its activity after 2 h reaction time. Moreover, a decrease in coke formation over the silane treated BEA catalyst was also observed. It is worth mentioning that  $C_{35+}$  yield over modified catalyst was negligible as compared to the one for parent catalyst. Gas composition analysis after 2 h reaction time in Figure. 31 shows no hydrogen formed in both parent and modified BEA catalysts. While it was reported that considerable amount of hydrogen was produced over metal oxide catalysts, which indicates the formation of coke [23, 60-62]. Problems involving dealumination caused in the presence of steam and coke formation were mitigated using silane treated zeolite catalysts. Major constituents of the gases produced were alkenes and alkanes in the case of BEA-zeolite. Molecular weight distribution curves in Figure. 32 showed full agreement with above mentioned results. A sharp increase in peak was observed in the lighter hydrocarbon area over silane treated BEA catalyst. The higher amount of the lighter hydrocarbon over silane treated catalysts showed less coke formation. Figure. 33 showed the physical appearance of liquid product after reaction over parent and the modified BEA zeolite catalyst. Light yellow color of product over silane treated catalyst results indicates the presence of lighter components.

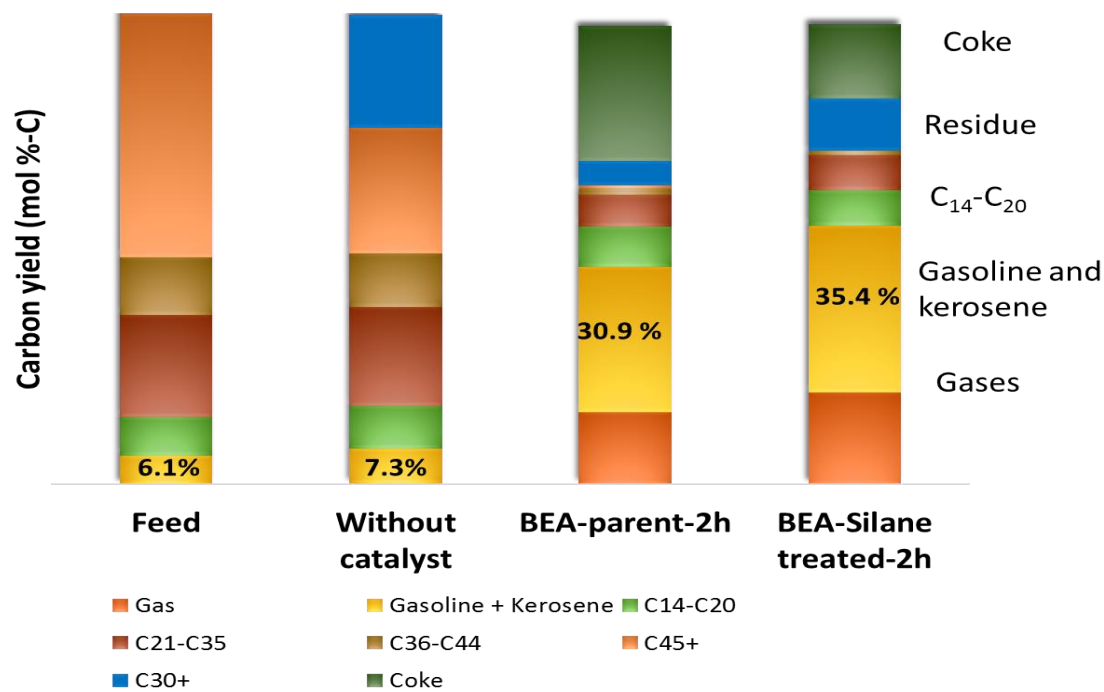


Figure 30. Carbon yield after 2 h reaction of AR with steam over BEA-parent and BEA-Liquid phase silane treated catalysts.

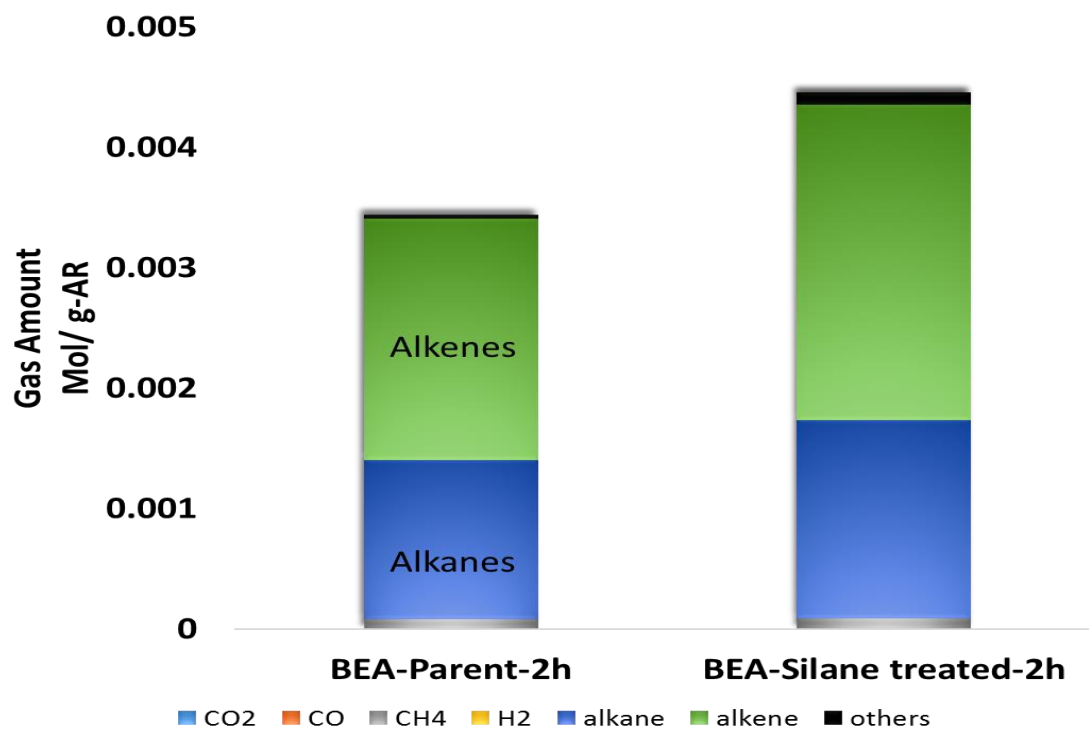


Figure 31. Gas composition (mol %) after 2 h reaction of AR with steam over BEA-parent and BEA-Liquid phase silane treated catalysts.

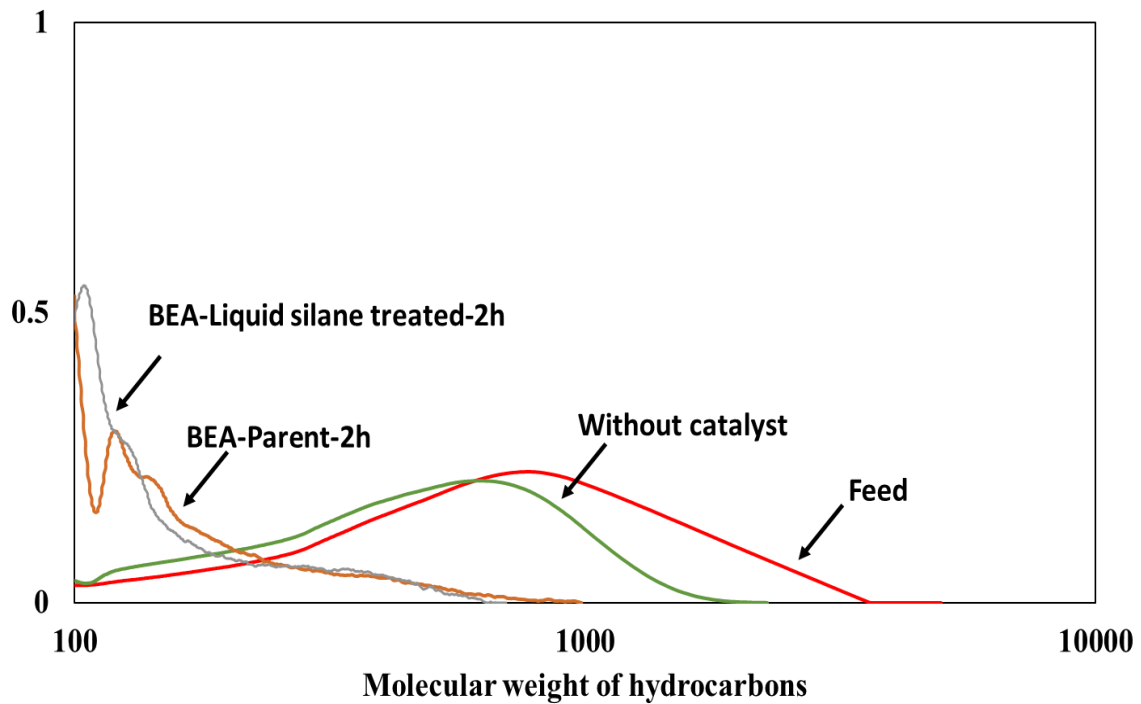


Figure 32. Molecular weight distribution of liquid product over BEA-Parent and BEA-Liquid silane treated catalysts after 2 h reaction time.



Figure 33. Physical appearance of liquid product after 2 h reaction time over (a) BEA-parent and (b) BEA-Liquid silane treated catalysts.

### 5.3 Effect of reaction time on cracking of AR

Stability of parent and silane treated BEA catalyst was measured after a prolonged reaction time for 4 h. Reaction test was repeated for 4 h over parent and silane treated catalyst and product distribution was carefully studied. Figure. 34 represents an increase in lighter component yield over silane treated BEA-zeolite catalyst. Gasoline ( $C_7-C_{13}$ ) yield increased up to 34.1 mol% as compared to 27 mol% over parent BEA-zeolite. Relatively less amount of coke formed over silane treated BEA catalyst showed partial

coverage of the external sites by silane compounds. Less amount of coke leads to the improved stability of catalyst and higher yield of lighter components. Gas composition analysis in Figure. 35 show a high percentage of hydrogen gas produced over the parent BEA catalyst after 4 h reaction, which indicates that after longer reaction time, significant amount of coke was deposited on the parent BEA catalyst while there was no hydrogen gas was formed over silane treated BEA catalyst, even after 4 h reaction time. Major gas constituents in the gas of silane treated zeolite were alkanes and alkenes. High percentage of alkenes was obtained over silane treated zeolite. Figure. 36 represents the better view of liquid product distribution according to their molecular weight. Large area under the graph of silane treated zeolite in the low molecular weight region showed a high percentage of lighter components.

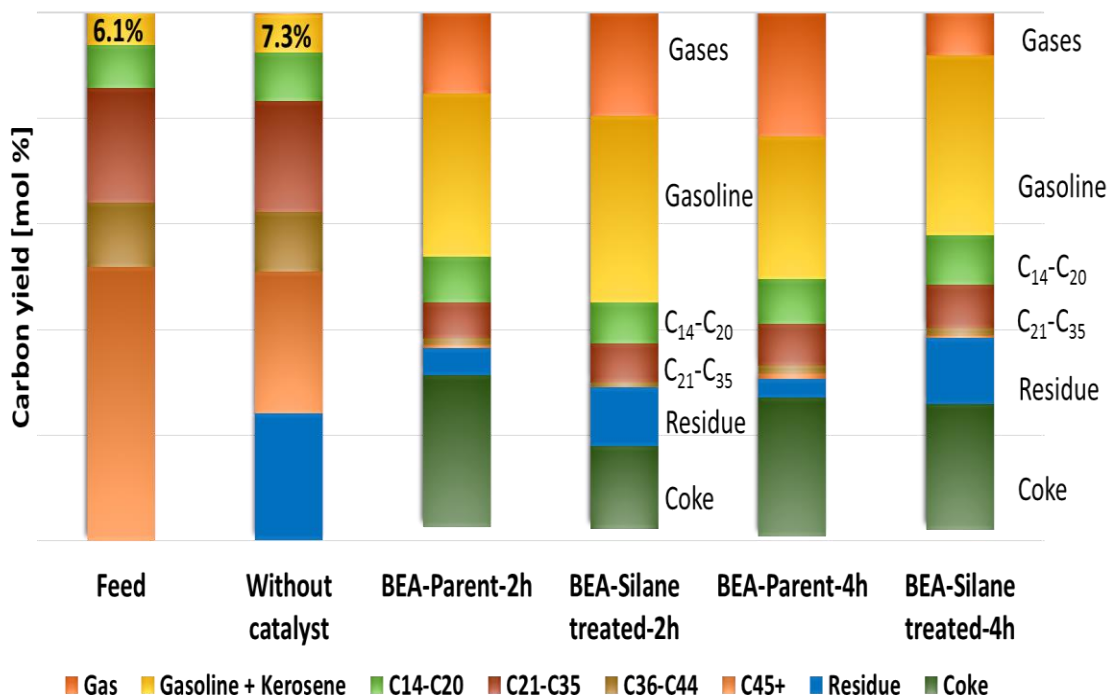


Figure 34. Physical appearance of liquid product after 4 h reaction time over (a) BEA-parent and (b) BEA-Liquid silane treated catalysts.

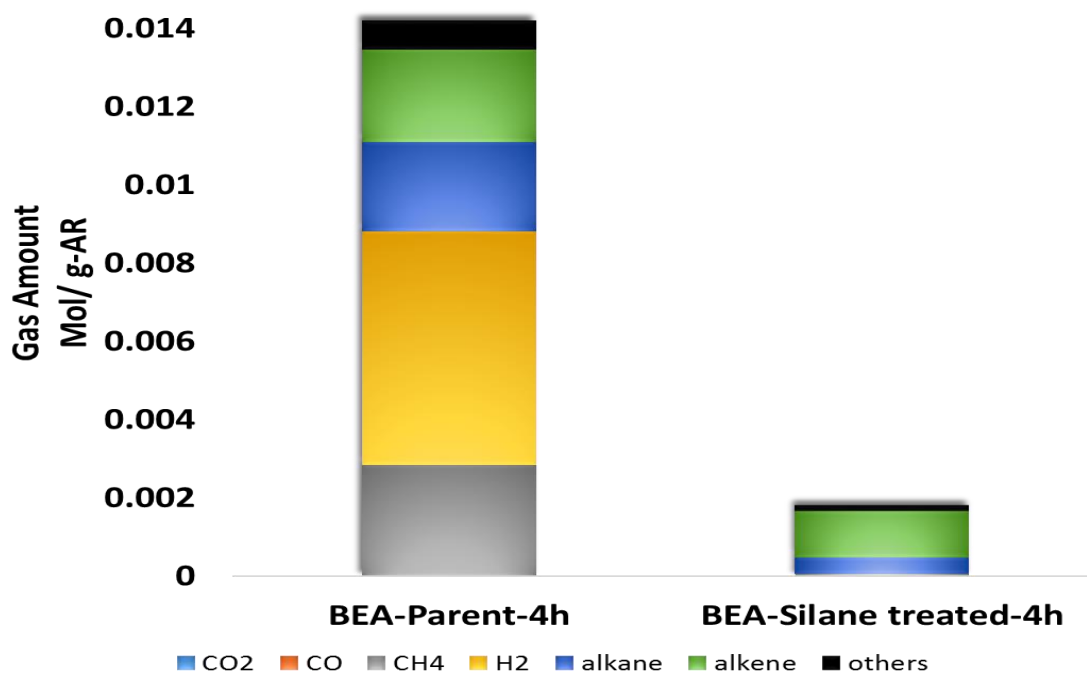
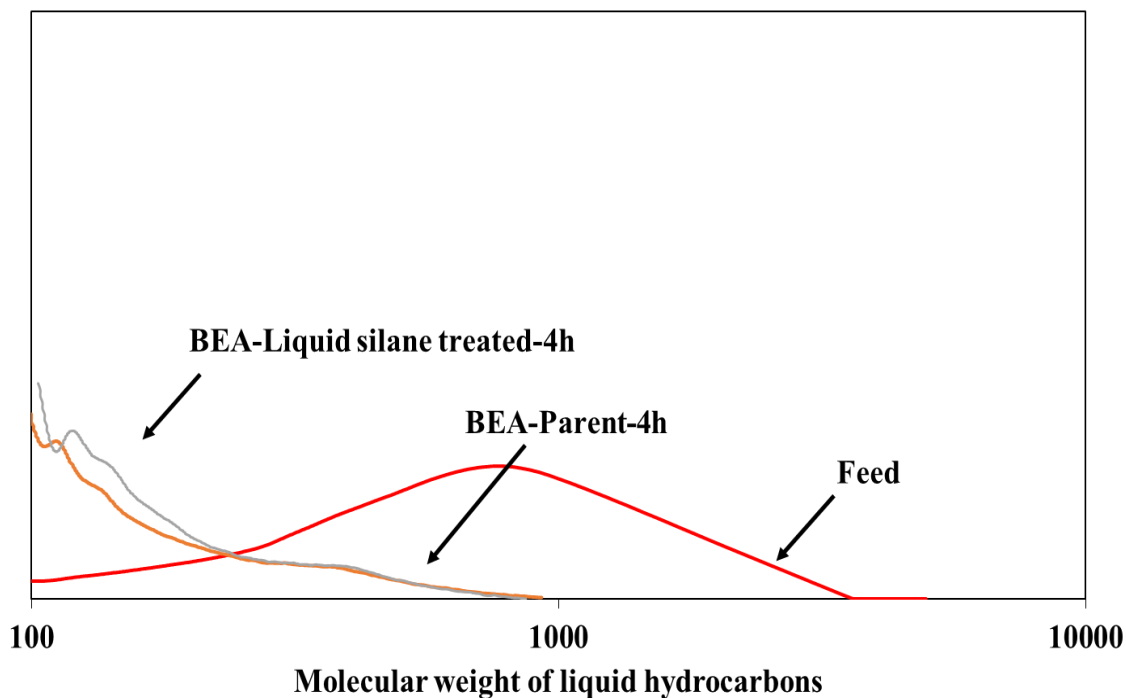


Figure 35. Gas composition (mol %) after 4 h reaction of AR with steam over BEA-parent and BEA-Liquid phase silane treated catalysts.



**Figure 36. Molecular weight distribution of liquid product over BEA-Parent and BEA-Liquid silane treated catalysts after 4 h reaction time.**

Change in the crystallinity of parent and a modified catalyst was studied from XRD patterns. Figure. 37 (XRD patterns) shows that the BEA catalyst retained its crystallinity, even after 2 h reaction and phase purity were still intact. Despite no structural changes were observed after 2 h for parent BEA catalyst, some changes in phase purity were clearly observed after 4 h reaction. Impure phase was appeared after a longer reaction time in parent catalyst, which indicates changes in the structure of zeolite. On the other hand, the silane treated BEA-catalyst exhibited stable structure even after 4 h. Silane compounds attached to the external surface of zeolite prevented the structure from the attack of water and made stable hydrophobic catalyst.

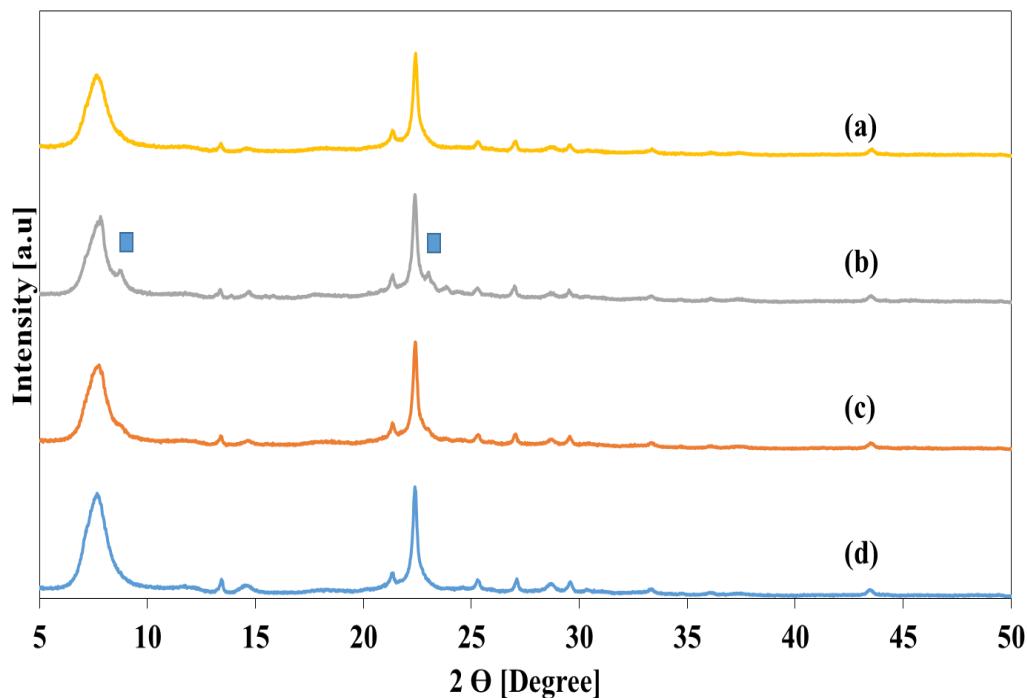


Figure 37. XRD patterns of (a) BEA-Vapor silane treated-4h (b) BEA-Parent-4h (c) BEA-Liquid silane treated-2h (d) BEA-Parent.

## 5.4 Comparison between Vapor phase and liquid phase silane treated catalyst

It was observed that high percentage of lighter component was obtained over vapor phase silane treated BEA catalyst as compare to liquid phase silane treated BEA catalyst. Reason may be the uniform coverage of catalyst surface when it was modified in vapor phase. In liquid phase there may be agglomeration of silane compound on catalyst surface. Uniformly modified surface more effectively repel the water molecules and make the catalyst more stable. Figure. 38. shows that after 2 h reaction remarkable increase in gasoline from 30.9 mol % over parent to 55.7 mol % over vapor silane treated catalyst. In the case of liquid silane treated catalyst this increase was up to 35.4 mol %.

Moreover, comparatively less coke formed in later case. When XRD patterns of both silane treated and parent catalysts was observed there was no considerable change in crystallinity was observed this indicates the stable structure after 2 h reaction. All three catalysts retained their crystallinity and phase purity. On contrary to this, after 4 h reaction XRD analysis showed structural changes in parent catalyst while vapor and liquid phase silane treated catalysts were stable. After 4 h reaction gasoline yield was higher over vapor phase silane treated as compare to parent and liquid silane treated catalysts. It was also observed that large percentage of hydrogen was produced over parent catalyst while no hydrogen was formed in both modified catalysts. Major constituent of gas product over silane treated catalysts were alkenes and alkanes.

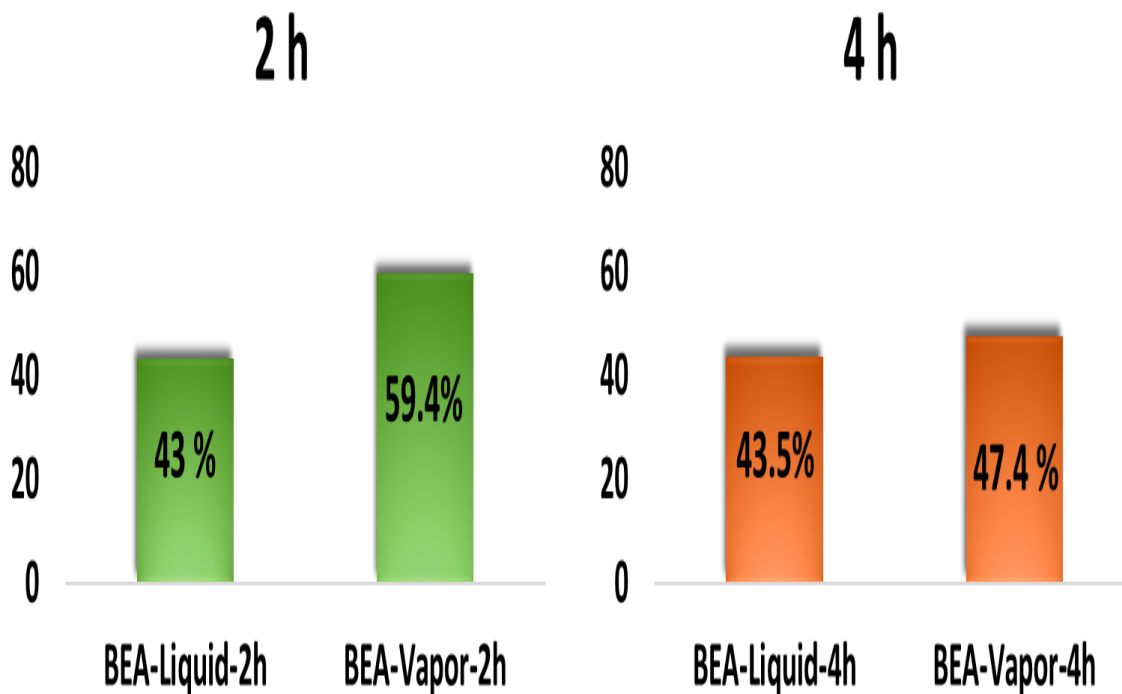
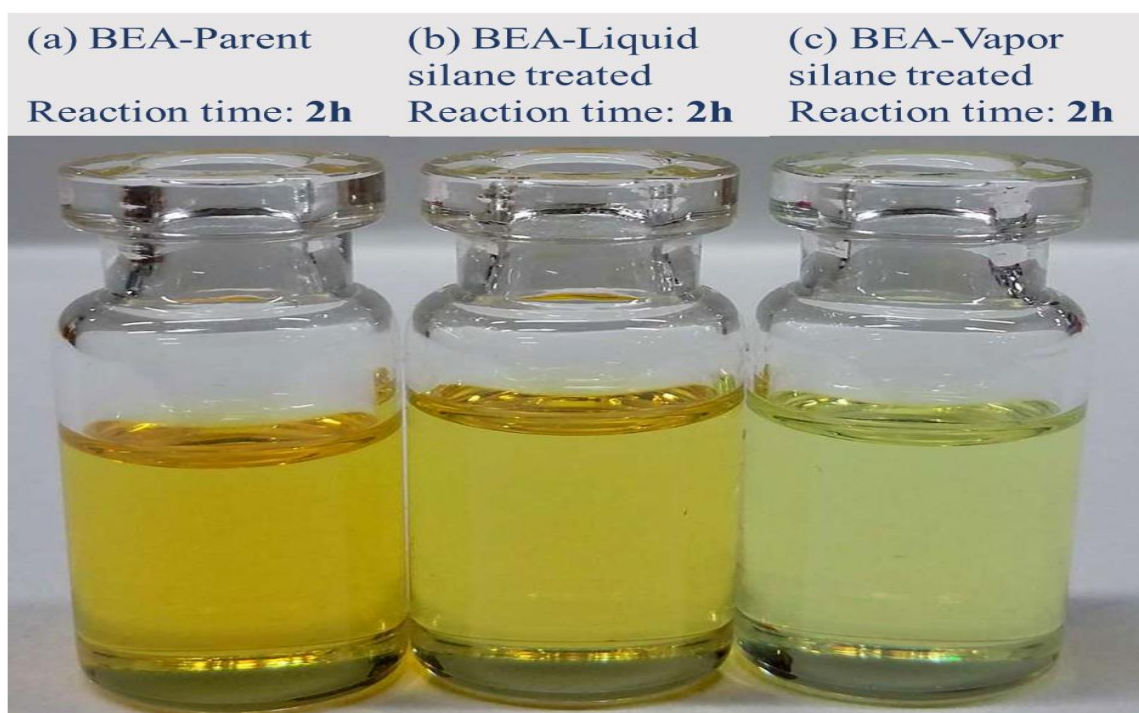


Figure 38. Comprison of lighter hydrocarbon yield over vapor silane treated and liquid silane treated catalysts for 2h and 4h reaction times.

Physical appearance of liquid product over all catalysts were observed in Figure 39 after 2 h and 4 h reaction. Lighter color was observed over vapor phase silane treated catalyst as compare to parent and liquid silane treated catalysts this indicates the lighter components were formed over vapor phase silane treated catalyst. This trend was observed in both 2 h and 4 h reaction time.



**Figure 39. Physical appearance of liquid product after 2 h reaction time over (a) BEA-parent (b) BEA-Liquid silane treated and (c) BEA-Vapor silane treated catalyst.**

## CHAPTER 6

### 6.1 Conclusions

Organosilane compound (triphenyl silane) was used to modify the external surface of beta zeolite catalysts.

Two different techniques i.e. vapor silane deposition and liquid silane deposition were used to modify the Beta catalyst. Both parent and modified BEA catalysts were characterized using XRD, NH<sub>3</sub>-TPD, FT-IR pyridine and N<sub>2</sub>-adsorption.

XRD patterns showed no change in crystallinity and phase purity of catalysts after modification. While NH<sub>3</sub>-TPD and FT-IR pyridine analysis showed decrease in acidity of silane treated BEA catalysts. Small increase in external surface was reported after silane treatment through both techniques.

Parent and silane treated BEA catalysts were tested in fixed-bed reactor for steam-assisted catalytic cracking of heavy oil for 2 h and 4 h reaction times.

Yield of gases, gasoline (C<sub>7</sub>-C<sub>13</sub>) and gas oil (C<sub>14</sub>-C<sub>20</sub>) over a vapor phase silane treated Beta zeolite catalyst were 11.6 mol %, 55.7 mol % and 3.7 mol % respectively for 2 h reaction time while negligible amount of C<sub>20+</sub> hydrocarbons were produced.

After 4 h reaction time, XRD analysis showed impure phase in BEA parent catalysts while there was no change in purity of silane treated BEA catalysts after reaction.

These findings indicate that organo-silane groups attached to the external surface of catalysts protect the surface from water attack (dealumination) and made the zeolite stable in the aqueous environment.

## **6.2 Recommendations**

Modified catalysts should also be test for cracking reactions in the presence of liquid water.

Different chain length of silane compounds may have

Study the effect of increasing reaction time on the stability of catalysts.

Different zeolite catalysts should be tested after modification.

Other modification routes such as impregnation of fluoride, phosphorus and lanthanum on zeolites should be studied for cracking reactions in the aqueous environment.

## References

1. Junaid, A.S.M., *Natural Zeolite Catalysts for the Integrated Cracking, Waterless Extraction and Upgrading of Oilsands Bitumen*. 2012, University of Alberta.
2. Birol, F., *World energy outlook 2010*. International Energy Agency, 2010.
3. Castañeda, L., J. Muñoz, and J. Ancheyta, *Combined process schemes for upgrading of heavy petroleum*. *Fuel*, 2012. **100**: p. 110-127.
4. Yen, T., *Structure of petroleum asphaltene and its significance*. *Energy Sources, Part A Recovery, Utilization, and Environmental Effects*, 1974. **1**(4): p. 447-463.
5. Yen, T.F. and G.V. Chilingarian, *Asphaltenes and asphalts*, 2. 2000: Elsevier.
6. Kulprathipanja, S., *Zeolites in industrial separation and catalysis*. 2010: Wiley Online Library.
7. Tago, T., et al., *Preparation for size-controlled MOR zeolite nanocrystal using water/surfactant/organic solvent*. *Topics in Catalysis*, 2009. **52**(6-7): p. 865-871.
8. Zhang, L., et al., *Crystallization and morphology of mordenite zeolite influenced by various parameters in organic-free synthesis*. *Materials Research Bulletin*, 2011. **46**(6): p. 894-900.
9. Lu, B., et al., *Control of crystal size of high-silica mordenite by quenching in the course of crystallization process*. *Microporous and mesoporous materials*, 2006. **95**(1): p. 141-145.
10. Hincapie, B.O., et al., *Synthesis of mordenite nanocrystals*. *Microporous and mesoporous materials*, 2004. **67**(1): p. 19-26.
11. Mao, Y., et al., *Morphology-controlled synthesis of large mordenite crystals*. *New Journal of Chemistry*, 2014.
12. Thomas, C.L., *Chemistry of cracking catalysts*. *Industrial & Engineering Chemistry*, 1949. **41**(11): p. 2564-2573.
13. Hyne, J., *Aquathermolysis: A Synopsis of Work on the Chemical Reaction Between Water (steam) and Heavy Oil Sands During Simulated Steam Stimulation*. 1986: AOSTRA Library and Information Service.
14. Clark, P. and J. Hyne, *Steam-oil chemical reactions: mechanisms for the aquathermolysis of heavy oil*. *Aostran J Res*, 1984. **1**(1): p. 15-20.
15. Maity, S., J. Ancheyta, and G. Marroquín, *Catalytic aquathermolysis used for viscosity reduction of heavy crude oils: A review*. *Energy & Fuels*, 2010. **24**(5): p. 2809-2816.
16. WU, C., et al., *Mechanism for reducing the viscosity of extra-heavy oil by aquathermolysis with an amphiphilic catalyst*. *Journal of Fuel Chemistry and Technology*, 2010. **38**(6): p. 684-690.
17. Yuanqing, W., et al., *Mechanism of catalytic aquathermolysis: influences on heavy oil by two types of efficient catalytic ions: Fe<sup>3+</sup> and Mo<sup>6+</sup>*, in *Energy Fuels*. 2010. p. 1502-10.
18. Clark, P.D., et al., *Studies on the effect of metal species on oil sands undergoing steam treatments*. *Aostran J Res*, 1990. **6**(1): p. 53-64.
19. Clark, P.D. and M.J. Kirk, *Studies on the upgrading of bituminous oils with water and transition metal catalysts*. *Energy & fuels*, 1994. **8**(2): p. 380-387.

20. Yi, Y., et al., *Change of asphaltene and resin properties after catalytic aquathermolysis*. Petroleum Science, 2009. **6**(2): p. 194-200.
21. Chen, Y., et al., *GC-MS used in study on the mechanism of the viscosity reduction of heavy oil through aquathermolysis catalyzed by aromatic sulfonic H<sub>3</sub>PMo<sub>12</sub>O<sub>40</sub>*. Energy, 2010. **35**(8): p. 3454-3460.
22. Chao, K., et al., *Laboratory experiments and field test of a difunctional catalyst for catalytic aquathermolysis of heavy oil*. Energy & Fuels, 2012. **26**(2): p. 1152-1159.
23. Li, W., J.-H. Zhu, and J.-H. Qi, *Application of nano-nickel catalyst in the viscosity reduction of Liaohe extra-heavy oil by aqua-thermolysis*. Journal of Fuel Chemistry and Technology, 2007. **35**(2): p. 176-180.
24. Hongfu, F., et al., *The study on composition changes of heavy oils during steam stimulation processes*. Fuel, 2002. **81**(13): p. 1733-1738.
25. Desouky, S., *Catalytic Aquathermolysis of Egyptian Heavy Crude Oil*.
26. Fan, H., Y. Zhang, and Y. Lin, *The catalytic effects of minerals on aquathermolysis of heavy oils*. Fuel, 2004. **83**(14): p. 2035-2039.
27. Olvera, J.N.R., et al., *Use of unsupported, mechanically alloyed NiWMoC nanocatalyst to reduce the viscosity of aquathermolysis reaction of heavy oil*. Catalysis Communications, 2014. **43**: p. 131-135.
28. Liu, Y. and H. Fan, *The effect of hydrogen donor additive on the viscosity of heavy oil during steam stimulation*. Energy & fuels, 2002. **16**(4): p. 842-846.
29. Chen, Y., et al., *The viscosity reduction of nano-keggin-K<sub>3</sub>PMo<sub>12</sub>O<sub>40</sub> in catalytic aquathermolysis of heavy oil*. Fuel, 2009. **88**(8): p. 1426-1434.
30. Chen, Y., et al., *GC-MS used in study on the mechanism of the viscosity reduction of heavy oil through aquathermolysis catalyzed by aromatic sulfonic H<sub>3</sub>PMo<sub>12</sub>O<sub>40</sub>*. Energy, 2010. **35**(8): p. 3454-3460.
31. XU, H.-x. and C.-s. PU, *Experimental study of heavy oil underground aquathermolysis using catalyst and ultrasonic*. Journal of Fuel Chemistry and Technology, 2011. **39**(8): p. 606-610.
32. Sharma, P., P. Rajaram, and R. Tomar, *Synthesis and morphological studies of nanocrystalline MOR type zeolite material*. Journal of colloid and interface science, 2008. **325**(2): p. 547-557.
33. Weitkamp, J. and L. Puppe, *Catalysis and zeolites: fundamentals and applications*. 1999: Springer.
34. Aly, H.M., M.E. Moustafa, and E.A. Abdelrahman, *Synthesis of mordenite zeolite in absence of organic template*. Advanced Powder Technology, 2012. **23**(6): p. 757-760.
35. Ravenelle, R.M., et al., *Stability of zeolites in hot liquid water*. The Journal of Physical Chemistry C, 2010. **114**(46): p. 19582-19595.
36. Bakare, I.A., et al., *Steam-assisted catalytic cracking of n-hexane over La-Modified MTT zeolite for selective propylene production*. Journal of Analytical and Applied Pyrolysis, 2015.

37. Maier, S.M., A. Jentys, and J.A. Lercher, *Steaming of zeolite BEA and its effect on acidity: a comparative NMR and IR spectroscopic study*. The Journal of Physical Chemistry C, 2011. **115**(16): p. 8005-8013.
38. Simon-Masseron, A., et al., *Influence of the Si/Al ratio and crystal size on the acidity and activity of HBEA zeolites*. Applied Catalysis A: General, 2007. **316**(1): p. 75-82.
39. Zapata, P.A., et al., *Silylated hydrophobic zeolites with enhanced tolerance to hot liquid water*. Journal of Catalysis, 2013. **308**: p. 82-97.
40. Weber, R., K. Möller, and C. O'Connor, *The chemical vapour and liquid deposition of tetraethoxysilane on ZSM-5, mordenite and beta*. Microporous and Mesoporous Materials, 2000. **35**: p. 533-543.
41. Zapata, P.A., et al., *Hydrophobic Zeolites for Biofuel Upgrading Reactions at the Liquid-Liquid Interface in Water/Oil Emulsions*. Journal of the American Chemical Society, 2012. **134**(20): p. 8570-8578.
42. Chen, N., *Hydrophobic properties of zeolites*. The Journal of Physical Chemistry, 1976. **80**(1): p. 60-64.
43. Zhao, X., et al., *Comprehensive study of surface chemistry of MCM-41 using <sup>29</sup>Si CP/MAS NMR, FTIR, pyridine-TPD, and TGA*. The Journal of Physical Chemistry B, 1997. **101**(33): p. 6525-6531.
44. Blasco, T., A. Corma, and J. Martínez-Triguero, *Hydrothermal stabilization of ZSM-5 catalytic-cracking additives by phosphorus addition*. Journal of catalysis, 2006. **237**(2): p. 267-277.
45. Ates, A., et al., *The role of catalyst in supercritical water desulfurization*. Applied Catalysis B: Environmental, 2014. **147**: p. 144-155.
46. Kamimura, Y., et al., *Synthesis of hydrophobic siliceous ferrierite by using pyridine and sodium fluoride*. Microporous and Mesoporous Materials, 2013. **181**: p. 154-159.
47. Caeiro, G., et al., *Stabilization effect of phosphorus on steamed H-MFI zeolites*. Applied Catalysis A: General, 2006. **314**(2): p. 160-171.
48. Damodaran, K., et al., *Modification of H-ZSM-5 zeolites with phosphorus. 2. Interaction between phosphorus and aluminum studied by solid-state NMR spectroscopy*. Microporous and mesoporous materials, 2006. **95**(1): p. 296-305.
49. Ritter, S., *Zeolites Don't Mind Hot Water*. 2012, AMER CHEMICAL SOC 1155 16TH ST, NW, WASHINGTON, DC 20036 USA.
50. Cejka, J., A. Corma, and S. Zones, *Zeolites and catalysis: synthesis, reactions and applications*. 2010: John Wiley & Sons.
51. Xu, R., et al., *Chemistry of zeolites and related porous materials: synthesis and structure*. 2009: John Wiley & Sons.
52. Muraza, O., et al., *Microwave-assisted hydrothermal synthesis of submicron ZSM-22 zeolites and their applications in light olefin production*. Microporous and Mesoporous Materials, 2015. **206**: p. 136-143.
53. Tago, T., et al., *Size-controlled synthesis of nano-zeolites and their application to light olefin synthesis*. Catalysis Surveys from Asia, 2012. **16**(3): p. 148-163.
54. Zheng, S., et al., *Influence of surface modification on the acid site distribution of HZSM-5*. The Journal of Physical Chemistry B, 2002. **106**(37): p. 9552-9558.

55. Karpov, S., et al., *Structure, hydrophobicity, and hydrothermostability of MCM-41 organo-inorganic mesoporous silicates silylated with dimethoxydimethylsilane and dichloromethylphenylsilane*. Russian Journal of Physical Chemistry A, 2013. **87**(11): p. 1888-1894.
56. Gao, N., et al., *Improvement of vapor-phase silylation and thermal stability of silylated MCM-22 zeolite*. Journal of Porous Materials, 2013. **20**(5): p. 1217-1224.
57. Shang, Y., et al., *Modification of MCM-22 zeolites with silylation agents: Acid properties and catalytic performance for the skeletal isomerization of *n*-butene*. Catalysis Communications, 2008. **9**(5): p. 907-912.
58. Sanhoob, M., et al., *Synthesis of ZSM-12 (MTW) with different Al-source: Towards understanding the effects of crystallization parameters*. Microporous and Mesoporous Materials, 2014. **194**: p. 31-37.
59. Sanhoob, M.A., et al., *Role of crystal growth modifiers in the synthesis of ZSM-12 zeolite*. Advanced Powder Technology, 2015. **26**(1): p. 188-192.
60. Funai, S., et al., *Recovery of useful lighter fuels from petroleum residual oil by oxidative cracking with steam using iron oxide catalyst*. Chemical Engineering Science, 2010. **65**(1): p. 60-65.
61. Fumoto, E., et al., *Recovery of Lighter Fuels by Cracking Heavy Oil with Zirconia–Alumina–Iron Oxide Catalysts in a Steam Atmosphere†*. Energy & Fuels, 2009. **23**(3): p. 1338-1341.
62. Fumoto, E., T. Tago, and T. Masuda, *Production of lighter fuels by cracking petroleum residual oils with steam over zirconia-supporting iron oxide catalysts*. Energy & fuels, 2006. **20**(1): p. 1-6.
63. Konno, H., et al., *Kinetics of *n*-hexane cracking over ZSM-5 zeolites—effect of crystal size on effectiveness factor and catalyst lifetime*. Chemical Engineering Journal, 2012. **207**: p. 490-496.
64. Konno, H., et al., *Characterization and catalytic performance of modified nano-scale ZSM-5 for the acetone-to-olefins reaction*. Applied Catalysis A: General, 2014. **475**: p. 127-133.
65. Mori, N., et al., *Deactivation of zeolites in *n*-hexane cracking*. Applied catalysis, 1991. **74**(1): p. 37-52.
66. Paweewan, B., P.J. Barrie, and L.F. Gladden, *Coking and deactivation during *n*-hexane cracking in ultrastable zeolite Y*. Applied Catalysis A: General, 1999. **185**(2): p. 259-268.
67. Corma, A., et al., *The role of different types of acid site in the cracking of alkanes on zeolite catalysts*. Journal of Catalysis, 1985. **93**(1): p. 30-37.
68. Abbot, J., *Role of Brønsted and Lewis acid sites during cracking reactions of alkanes*. Applied Catalysis, 1989. **47**(1): p. 33-44.
69. Gounder, R., *Hydrophobic microporous and mesoporous oxides as Brønsted and Lewis acid catalysts for biomass conversion in liquid water*. Catalysis Science & Technology, 2014. **4**(9): p. 2877-2886.
70. Corma, A., J. Mengual, and P.J. Miguel, *Steam catalytic cracking of naphtha over ZSM-5 zeolite for production of propene and ethene: Micro and macroscopic implications of the presence of steam*. Applied Catalysis A: General, 2012. **417**: p. 220-235.

71. Corma, A., J. Mengual, and P.J. Miguel, *Stabilization of ZSM-5 zeolite catalysts for steam catalytic cracking of naphtha for production of propene and ethene*. Applied Catalysis A: General, 2012. **421**: p. 121-134.
72. Cambor, M.A., A. Corma, and S. Valencia, *Synthesis in fluoride media and characterisation of aluminosilicate zeolite beta*. Journal of Materials Chemistry, 1998. **8**(9): p. 2137-2145.
73. Muraza, O., *Hydrous pyrolysis of heavy oil using solid acid minerals for viscosity reduction*. Journal of Analytical and Applied Pyrolysis, 2015.
74. Muraza, O., et al., *Selective catalytic cracking of n-hexane to propylene over hierarchical MTT zeolite*. Fuel, 2014. **135**: p. 105-111.

## Vitae

**Name:** Umer Khalil Chaudhry

**Nationality:** Pakistani

**Date of Birth:** Dec 25, 1987

**Email:** [umerkhalilch@gmail.com](mailto:umerkhalilch@gmail.com)

**Address:** Lahore, Pakistan

---

**Academic** **Masters of Science in Chemical Engineering**

**Background:** Sep 13 – Nov 15

King Fahd University of Petroleum & Minerals, Saudi Arabia

**Bachelor of Science in Chemical Engineering**

Dec 07 – May 12

University of the Punjab, Lahore Pakistan

---

**Achievements** Publication of two research papers in high impact factor IS journals.

Secured research internship in Hokkaido University Japan.

---

**Publications** U.Khalil et al ‘Robust surface-modified Beta zeolite for selective production of lighter fuels by steam-assisted catalytic cracking from heavy oil’ Fuel 168 (2016) 61-67

U.Khalil et al ‘Production of lighter hydrocarbons by steam-assisted catalytic cracking of heavy oil over silane treated Beta zeolite’. Energy & Fuel

---

**Seminars and volunteer work** Presentation on ‘Stability of Mordenite zeolite catalysts in hot Liquid water’.

Lab instructor: Fluid mechanics laboratory.